Quaternary geology of the southern Core Zone area, Quebec and Newfoundland and Labrador

J.M. Rice[1*], R.C. Paulen[1], M. Ross[2], M.B. McClenaghan[1], and H.E. Campbell[3]

Rice, J.M., Paulen, R.C., Ross, M., McClenaghan, M.B., and Campbell, H.E., 2023. Quaternary geology of the southern Core Zone area, Quebec and Newfoundland and Labrador; in *Surficial geology of northern Canada: a summary of Geo-mapping for Energy and Minerals program contributions, (ed.) I. McMartin; Geological Survey of Canada, Bulletin 611, p 221–265. https://doi.org/10.4095/331426*

Abstract: The complex glacial geomorphology of east-central Quebec and western Labrador has resulted in conflicting ice-sheet reconstructions, leaving many questions regarding the behaviour of large ice sheets within their inner regions. Specifically, the ice-flow chronology and subglacial conditions remain poorly constrained. To address this, surficial geology investigations were conducted across the border of Quebec and Labrador. A complex glacial history consisting of five ice-flow phases influenced by regional ice-stream dynamics was identified, including a near-complete ice-flow reversal. During each ice-flow phase, the subglacial thermal conditions fluctuated both spatially and temporally, resulting in palimpsest glacial dispersal patterns. Deglacial ages from samples collected as part of this research confirm deglaciation occurred relatively rapidly around 8 ka. The results of this work lead to a better understanding of the glacial history of an inner region of the Laurentide Ice Sheet and have important implications for mineral exploration in the southern Core Zone area.

Résumé : La géomorphologie glaciaire complexe du centre est du Québec et de l'ouest du Labrador a donné lieu à des reconstitutions conflictuelles de l'inlandsis, soulevant de nombreuses questions sur le comportement des grandes nappes glaciaires dans leurs régions internes. Plus précisément, la chronologie de l'écoulement glaciaire et les conditions sous-glaciaires demeurent mal définies. Afin de répondre à ces questions, des études en géologie des formations superficielles ont été menées à la limite entre le Québec et le Labrador. Une histoire glaciaire complexe composée de cinq phases d'écoulement glaciaire influencées par la dynamique régionale des courants glaciaires a été déterminée, y compris une inversion presque complète de l'écoulement des glaces. Au cours de chaque phase d'écoulement glaciaire, les conditions thermiques sous-glaciaires ont fluctué à la fois dans l'espace et dans le temps, ce qui a entraîné des configurations de dispersion glaciaire palimpsestes. Les âges de la déglaciation provenant des échantillons prélevés dans le cadre de cette recherche confirment que le retrait glaciaire s'est produit de façon relativement rapide vers 8 ka. Les résultats de ces travaux améliorent notre compréhension de l'histoire glaciaire d'une région intérieure de l'Inlandsis laurentidien et ont des implications importantes pour l'exploration minérale dans la région sud de la Zone noyau.

[1]Geological Survey of Canada, 601 Booth Street, Ottawa, Ontario K1A 0E8
[2]Department of Earth and Environmental Sciences, University of Waterloo, 200 University Avenue W., Waterloo, Ontario N2L 3G1
[3]Geological Survey, Department of Natural Resources, Government of Newfoundland and Labrador, P.O. Box 8700, St. John's, Newfoundland and Labrador A1B 4J6
*Corresponding author: J.M. Rice (email: jessey.rice@nrcan-rncan.gc.ca)

INTRODUCTION

The geologically complex region straddling the border of east-central Quebec and western Labrador (Fig. 1) has an unresolved ice-flow chronology with contradicting relative ages (e.g. Veillette et al., 1999; Jansson et al., 2002) and few geochronological constraints on the timing of ice-margin retreat (e.g. Carlson et al., 2007; Ullman et al., 2016; Dubé-Loubert et al., 2018; Dalton et al., 2020). Prior to this research, only small-scale (1:1 000 000) surficial maps and sparse field-based data sets were available. The lack of geoscience data largely stems from the vastness and remoteness of the region, making it difficult to collect field-based data and constrain numerical models of the Laurentide Ice Sheet (LIS). These models predict a low probability of warm-based conditions and limited subglacial erosion within this region (e.g. Tarasov and Peltier, 2004; Stokes et al., 2012; Melanson et al., 2013), but are at odds with empirical evidence of a migrating ice divide and observations of significant glacial dispersal distances, typically associated with warm-based subglacial conditions (e.g. Klassen and Thompson, 1993). Developing a better understanding of the relative chronology and erosional intensity of ice-flow events, and the resulting glacial dispersal patterns, will offer important insights into ice-sheet dynamics and provide a beneficial framework for drift prospecting in glaciated terrains. The region is of particular interest, as glacial dispersal patterns could help refine bedrock geology in regions where bedrock outcrops are sparse (Fig. 2; Corrigan et al., 2015, 2016, 2018; McClenaghan et al., 2017). This study provides an extensive review of previous work in the region and presents a new ice-flow chronology and resulting glacial dispersal patterns that were developed through detailed surficial mapping and till-provenance studies conducted during the Northeast Quebec–Labrador Surficial Mapping activity of the Hudson–Ungava project undertaken as part of the second phase of the Geo-mapping for Energy and Minerals (GEM-2) program.

Previous work

Ice-sheet reconstruction

Ice-flow histories

Geological Survey of Canada (GSC) geologist A.P. Low was the first to conduct geological fieldwork in the southern Hudson–Ungava region. Based on the radial pattern of outcrop-scale ice-flow indicators measured during his expedition, he inferred the region was an area of significant ice accumulation, characterized by outward ice flow in all directions (i.e. an ice-outflow centre) and also the centre for ice-sheet recession (Low, 1896). The central Quebec–Labrador region is now well established as one of the largest regions of ice accumulation and dispersal of the LIS, commonly referred to as the Quebec–Labrador dome (Kleman et al., 2002; Jansson et al., 2003; Occhietti et al., 2004; Stokes et al., 2012), although exact areas of inception and early growth are unknown (e.g. Dyke and Prest, 1987). Historically, this region has also been referred to as the 'New Quebec dome' (Hillaire-Marcel et al., 1981; Vincent, 1989; Roy et al., 2015).

This region is characterized by a U-shaped boundary between streamlined glacial landforms converging toward Ungava Bay and radiating away, defined by a relatively sharp boundary (Fig. 3a). This pattern was interpreted by Wilson et al. (1953) and Douglas and Drummond (1955) as the position of a major ice divide of the Quebec–Labrador sector of the LIS. Hughes (1964), in contrast, interpreted the U-shaped boundary as the result of ice flow into Ungava Bay being younger than the radial flow in at least a part of the boundary area and, hence, did not necessarily indicate the location of a divide. Despite this, the divide location was continuously used for decades during subsequent ice-flow reconstructions, at least along its eastern arm (e.g. Prest, 1970; Fulton and Hodgson, 1979; Dyke et al., 1982).

Detailed field investigations of the region began in the early 1980s, when Klassen and Bolduc (1984) reported an old ice-flow event to the northeast, during fieldwork south of the Smallwood Reservoir, near Churchill Falls (Fig. 1). This early work was followed up by a larger field project led by Klassen and Thompson (1987, 1988, 1989, 1993) across western Labrador and parts of east-central Quebec. During this research project, over 300 striation measurements, supplemented by glacial erratic tracing and landform analysis, were used to identify five ice-flow phases that occurred over a large region of western Labrador and east-central Quebec (Fig. 3b). The oldest ice-flow phase (event I) was to the northeast, with striation evidence recorded within the study area and as far as 300 km northeast to the Labrador coast. Klassen and Thompson (1993) used northeast dispersal of different bedrock lithological units to indicate that this ice-flow phase affected all of Labrador but found little evidence of event I in western Labrador or east-central Quebec, where associated early-phase ice-flow vectors become indistinguishable from later ice-flow trajectories. Klassen and Thompson (1993) suggested that during event I, the ice divide was located to the southwest of Churchill Falls (*see* Fig. 1 for location), somewhere north of the St. Lawrence River, in a position much farther south than during later ice-flow phases, which they used as evidence to indicate event I occurred early during, or prior to, the Wisconsinan Glaciation. Following event I, the ice divide migrated north and was oriented southeast, resulting in ice flowing radially to the southwest, east-southeast, and east-northeast (event II), which episode was attributed to the last glacial maximum (LGM; Fig. 3b). The oriented glacial landforms converging toward Ungava Bay (Fig. 3a) were attributed to event III, with northwest ice flows that propagated from an ice divide located somewhere near Schefferville, all the way to Ungava Bay. Crosscutting landforms and striations were used as evidence that event III was followed by a younger, radial ice-flow

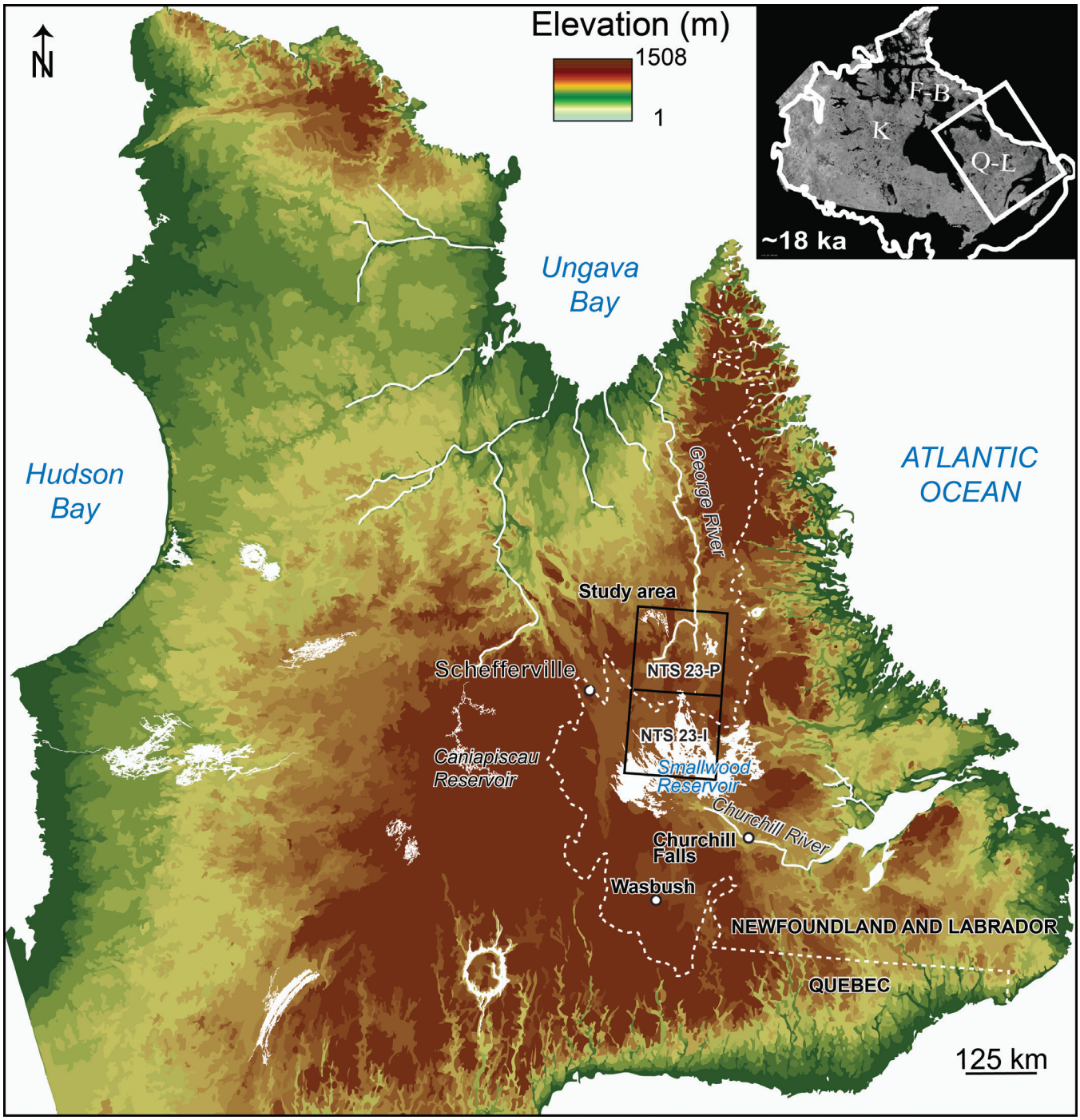

Figure 1. Location of the study area (black box), straddling the provincial border of Quebec and Newfoundland and Labrador (white dashed line). The inset map shows the extent of the Laurentide Ice Sheet during the last glacial maximum (~18 ka ^{14}C BP) outlined by a thick white line showing major ice domes, the Keewatin (K) in the west, Foxe–Basin (F-B) in the north, and Quebec–Labrador (Q-L) in the east (*after* Dyke, 2004). Base map is from Canadian Digital Elevation Model data downloaded from <https://open.canada.ca/data/en/dataset/7f245e4d-76c2-4caa-951a-45d1d2051333>.

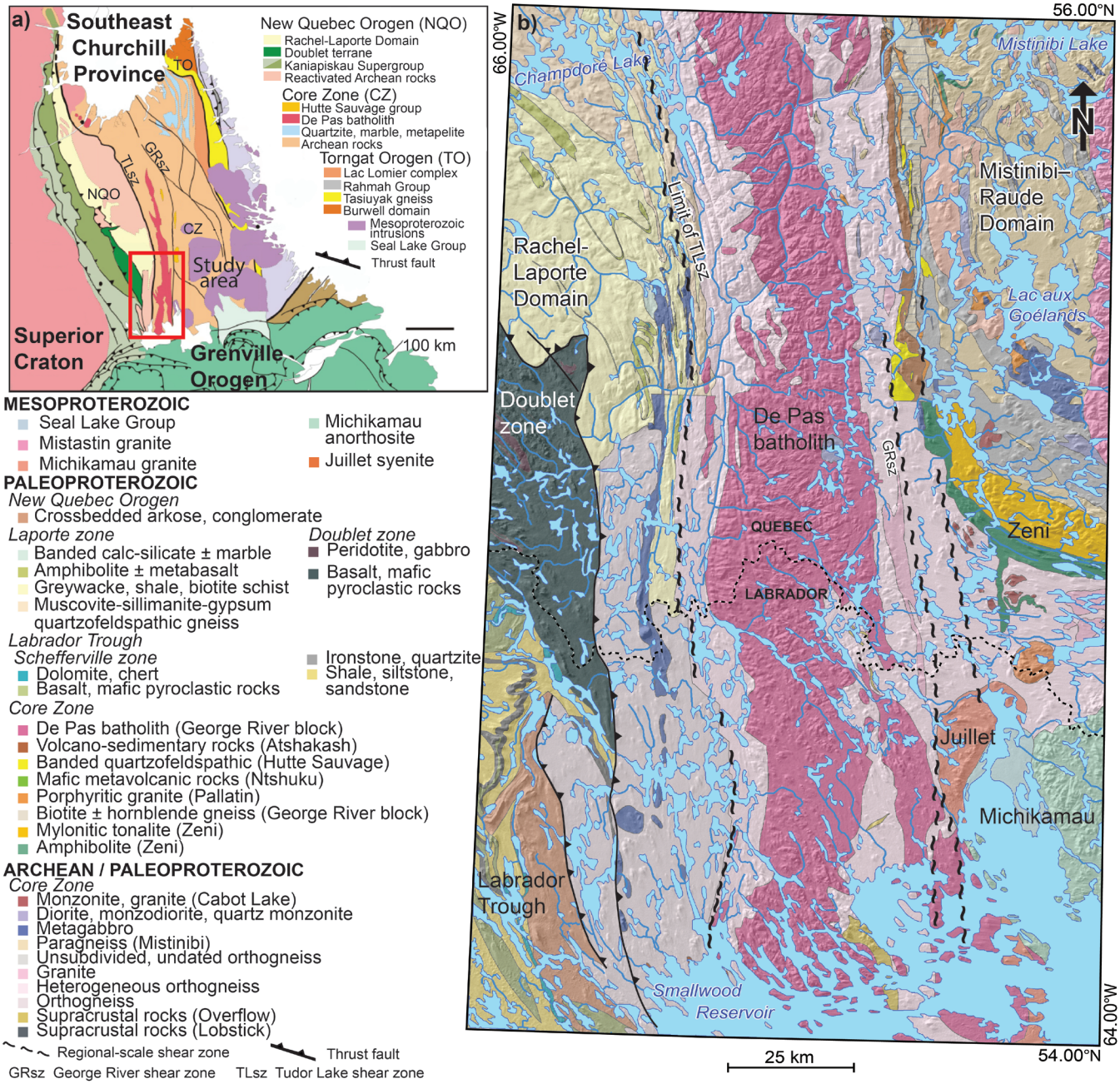

Figure 2. **a)** Simplified bedrock geology of the Core Zone within Quebec and Labrador (*modified from* James et al., 2003). **b)** Simplified bedrock geology of the study area (*modified from* Sanborn-Barrie, 2016; Corrigan et al., 2018); major bedrock formations are indicated on the left.

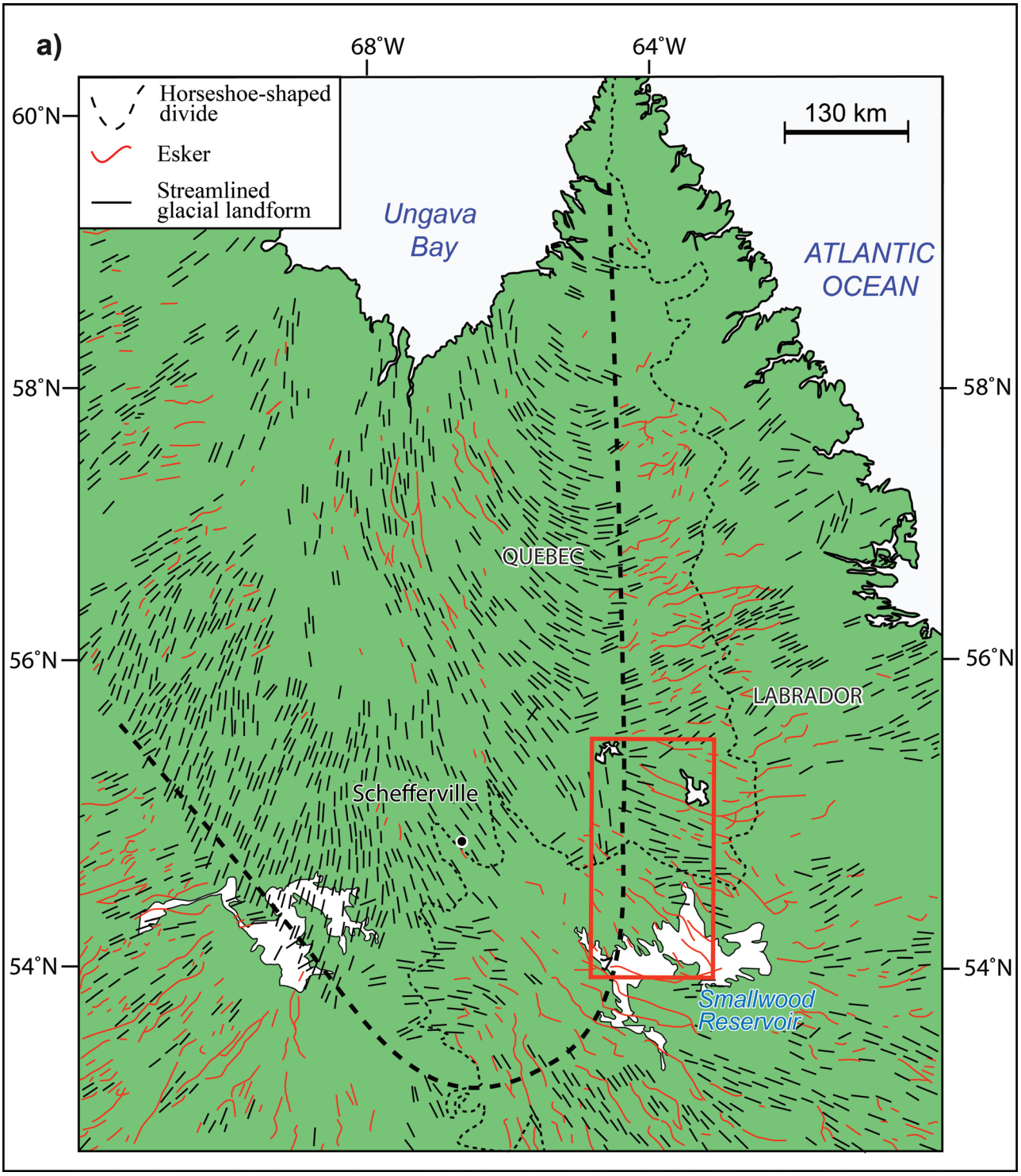

Figure 3. a) Map of east-central Quebec and western Labrador showing subglacial streamlined landforms and eskers with the U-shaped boundary as identified by Clark et al. (2000) indicated by the dashed line. This 'horseshoe' unconformity separates converging landforms into Ungava Bay from landforms oriented in the opposite direction. The study area is indicated by the red box. Landforms are from Fulton (1995)

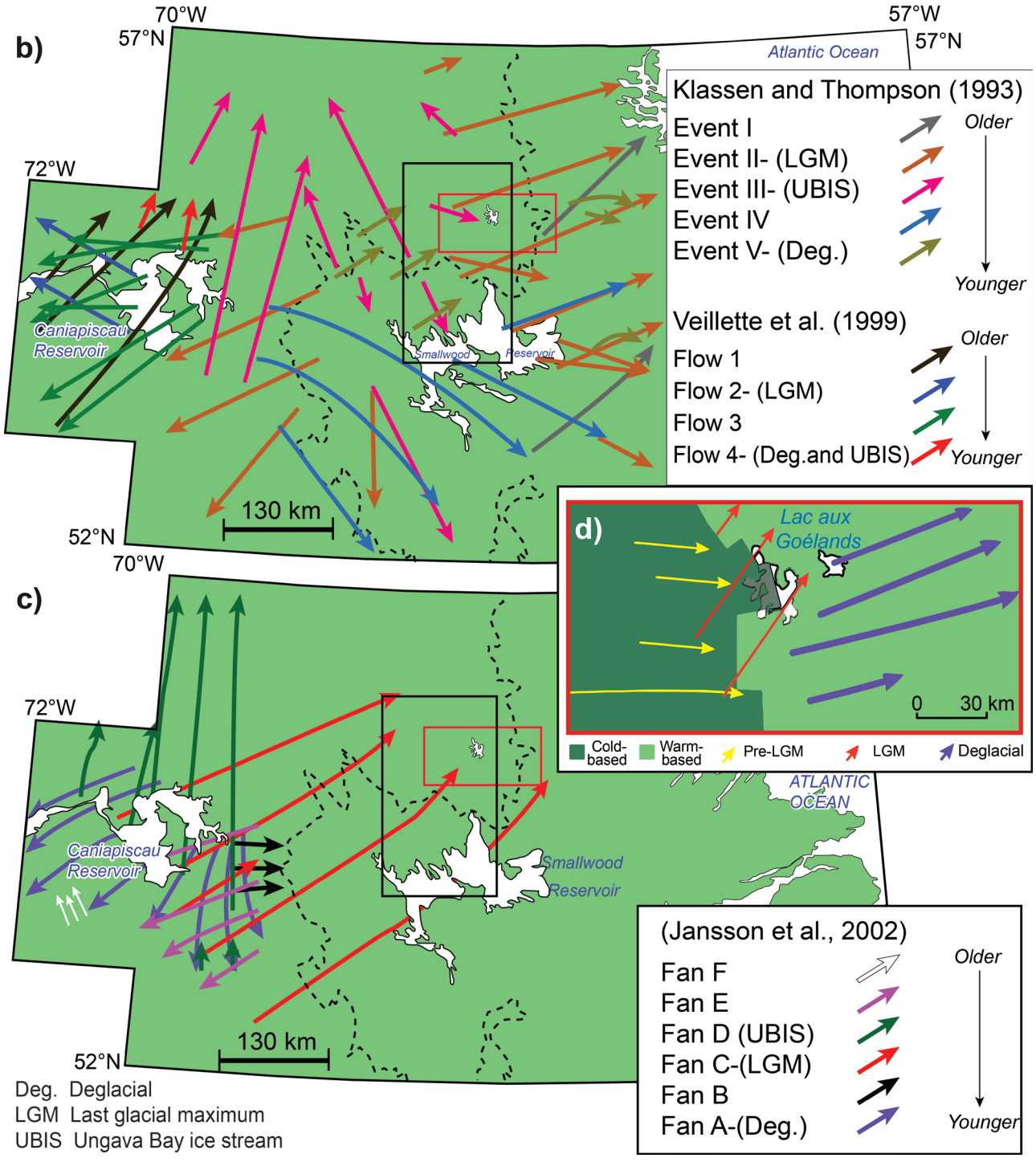

Figure 3. (cont.) b) Ice-flow reconstructions of Klassen and Thompson (1993) and Veillette et al. (1999) for the surrounding region; five and four ice-flow phases were identified, respectively. The study area is outlined in black, and location of (d) outlined in red. **c)** Ice-flow reconstruction of Jansson et al. (2002). **d)** Ice-flow reconstruction from fieldwork conducted south of Lac aux Goélands by Clarhäll and Jansson (2003), with their two earliest ice flows showing a chronology conflicting with that of Klassen and Thompson (1993) and Veillette et al. (1999) (*modified from* Rice et al., 2019).

phase (event IV) that propagated somewhere near the Caniapiscau Reservoir, with ice flowing to the southeast south of the Smallwood Reservoir and changing to the east, then northeast, north of the Smallwood Reservoir (Fig. 3b). These four main regional-scale ice-flow events were followed by a more localized, late-glacial event represented by fine, shallow striae indicating a northeast ice flow to the north of the Smallwood Reservoir and eastward ice flows, influenced more locally by topography, toward the Labrador coast (Fig. 3b). Later work by Liverman and Vatcher (1992, 1993), using surficial mapping and till sampling in the Schefferville region, supported the reconstruction of Klassen and Thompson (1993), with only some local variations in late ice-flow phases caused by topographic highs.

In addition to their relative ice-flow chronology, Klassen and Thompson (1993) investigated drift composition and glacial-erratic dispersal patterns. Through their work, they concluded that four of the ice-flow events accounted for the bulk of the glacial sediment dispersal: event I (northeast), event II (east/southeast/northeast), event III (northwest), and event IV (southeast/east/northeast).

Whereas Klassen and Thompson (1993) focused their work largely on an area east of the U-shaped boundary, Veillette et al. (1999) investigated the central and southwestern parts of the boundary along the Caniapiscau Reservoir, which allowed inspection of large areas of pristine, freshly exposed bedrock surfaces by boat, thus providing exceptional conditions for a detailed analysis of striated surfaces not found under standard field conditions. This work provided additional evidence, both in the striation and landform records, in support of the Hughes (1964) interpretation that claimed the U-shaped boundary was the capture limit of the warm-based Ungava Bay ice-flow events (i.e. that the boundary was an unconformity, not a divide). It also generally supported the ice-flow reconstruction for the area to the east proposed by Klassen and Thompson (1993). Within the Caniapiscau Reservoir area, Veillette et al. (1999) also identified a presumed, pre-Wisconsinan ice-flow event, citing north-northeast striated surfaces that are stained by a ferromanganese varnish and truncated by unstained striated surfaces formed by subsequent ice-flow phases. Klassen and Thompson (1993) had also found rare occurrences of an 'old' north-northeast ice flow on striated surfaces, which they attributed to an ice mass located somewhere in the Laurentian Highlands, north of the St. Lawrence River. Further evidence of possible pre-Wisconsinan ice-flow events includes the suspected pre-Wisconsinan till deposits reported in the Wabush area approximately 200 km southwest of the current study area (Fig. 1) by Klassen et al. (1988). Additionally, Granberg and Krishnan (1984) reported peat buried beneath 18 m of glaciofluvial sediments, which were overlain by till and found on the lee side of a steep bedrock scarp near Schefferville. However, wood from the peat layer yielded an age of 24 250 ± 600 ^{14}C years BP, indicating the region was ice-free near the end of the Middle Wisconsinan. However, no other data on pre-Late Wisconsinan sediments have been published for the region, and older pre-LGM, conventional radiocarbon dates should be interpreted with caution (e.g. Reyes et al., 2020). The hypothesis of an older (i.e. prior to Marine Isotope Stage (MIS) 5a) glaciation that would have originated from the Laurentian Highlands is speculative, and evidence of interglacial deposits remains limited to only a few observations.

Jansson et al. (2002) disagreed with the glacial reconstructions of Hughes (1964), Klassen and Thompson (1993), and Veillette et al. (1999) and instead suggested that the ice centre, at the start of the ice-margin retreat, was located just south of Ungava Bay (purple arrows in Fig. 3c). Jansson et al. (2002) used aerial photograph interpretations and fieldwork in the Caniapiscau Reservoir region to support their findings that ice flowed radially from the cold-based ice centre as the ice dome began to shrink. They suggested cold-based glacial conditions preserved landforms (associated with pre-LGM phase; black arrows in Fig. 3c) in the interior of the Quebec–Labrador region (dark green region in Fig. 3d). Follow-up work by Clarhäll and Jansson (2003) near Lac aux Goélands supported a change in subglacial dynamics that resulted in the preservation of older landforms (fan B in Fig. 3c and pre-LGM flow in Fig. 3d) under cold-based conditions during later ice-flow phases (fan C in Fig. 3c and LGM flow in Fig. 3d), conflicting with the ice-flow reconstruction of Klassen and Thompson (1993) and Veillette et al. (1999; Fig. 3b).

More recently, just north of the current study area, Dubé-Loubert (2019) reported detailed striation and landform evidence for an old ice-flow phase to the northeast, similar in orientation to event I of Klassen and Thompson (1993) and the oldest flow of Veillette et al. (1999). Additionally, Dubé-Loubert (2019) indicated that an ice divide formed along the George River valley and separated flow to the west-northwest on the western side of the river from ice flow to the east-northeast on the eastern side. This divide was inferred to have been active during the LGM, as previously suggested by Dyke and Prest (1987). Dubé-Loubert (2019) interpreted at least the eastern arm of the U-shaped boundary as an ice-divide position. How far south this divide extended is currently undefined. Dubé-Loubert (2019) also indicated that the landscape to the west of the divide consisted of a mosaic of landform assemblages from different ice-flow phases, with the youngest phase related to highly dynamic ice streams flowing north-northwest toward Ungava Bay. East of the divide, older ice-flow phases are crosscut by ice streaming associated with the Kogaluk (Strange Lake) ice stream (Margold et al., 2015). These results coupled with the abundance of ^{10}Be and ^{26}Al indicated that only small patchy regions were sustained under cold-based conditions throughout the last glaciation (Dubé-Loubert, 2019).

Ice-margin retreat

Early work confining the pattern and timing of ice-margin retreat in the Quebec–Labrador region focused on ^{14}C dating of material from raised beaches and reconstruction of isostatically tilted strandlines (Ives, 1958, 1960a, b; Matthews, 1961). From this work, it was suggested that the ice sheet fragmented into small ice caps during deglaciation. Subsequent work by Lauriol and Gray (1987) analyzing the distribution and orientation of eskers across the region supported the separation of the ice sheet into smaller ice masses during deglaciation. Clark et al. (2000) also supported ice-sheet fragmentation into smaller ice caps. These small ice caps would have been required to block meltwater drainage and allow for the formation of the proglacial lakes identified across Quebec and Labrador. Additionally, they suggested the retreat pattern was highly asymmetrical, with rapid southern retreat toward a cold-based ice centre, causing the centre to migrate approximately 500 km to the north from its earlier LGM position (around lat. 51°N), while continuously maintaining cold-based conditions during retreat. This northward migration was interpreted as the result of a thinning cold-based ice mass that eventually fragmented and disappeared about 5 ka ^{14}C BP, preserving the existing glacial landforms under cold-based conditions. Later work by Ullman et al. (2016) suggested a similar rapid ice-margin retreat as indicated from ^{10}Be deglacial ages from large erratic boulders along an approximately 400 km long transect (Fig. 4).

Glacial lake reconstructions and constraints on deglaciation

During ice-margin retreat of the Quebec–Labrador sector, many glacial lakes formed at the margins of the retreating ice mass (e.g. Clark et al., 2000; Dyke, 2004). Within the study area, drainage to the north was blocked in the George River and Rivière à la Baleine valleys (GR and RlB, respectively, on Fig. 4), creating glacial lakes Naskaupi and McLean, respectively (Ives 1960a, b; Barnett and Peterson, 1964; Barnett, 1967; Clark and Fitzhugh, 1990; Dubé-Loubert et al., 2018). Lake Naskaupi was first identified from its raised shorelines by an early twentieth century explorer (Prichart, 1911) and was formally named ‘Lake Naskaupi’ by Ives (1958, 1960a). Five lake levels (N1–N5) were described in detail (Henderson, 1959; Matthews, 1961; Barnett and Peterson, 1964). In the Lac aux Goélands area, Peterson (1965, Fig. IIIb) mapped the N2 levels as far south as latitude 55°30′N. As the drainage divide is just south of this area, this extent required ice dams to the south and west to prevent drainage. Recent investigations have confirmed the first four lake levels for Lake Naskaupi (N1–N4), with minor, transient stages between them (Dubé-Loubert and Roy, 2017). The main lake level (N2') is interpreted to have occupied two basins that were separated by a block of cold-based ice (Dubé-Loubert and Roy, 2017). The southern basin, which extended into the northeastern part of the study area, had an average depth of 50 m and formed distinct shorelines.

In the northwestern part of the region, another glacial lake inundated the study area and was named ‘McLean’ by Wallace (1932) after the Hudson Bay Company employee J. McLean, who first recognized the shorelines. The timing of lake inundation is unknown but occurred likely around the same time as the maximum extent of Lake Naskaupi (N2'). During N2' (472 m), Lake McLean, in the Rivière à la Baleine valley (Fig. 4), was periodically connected to Lake Naskaupi via several overflow channels, with overflow going into Lake Naskaupi north of the study area (Dubé-Loubert and Roy, 2017). Five levels were initially mapped for glacial Lake McLean (Mc1–Mc5), with its main stage (Mc2) evolving independently of Lake Naskaupi (Ives, 1960b). The shorelines of Lake McLean recorded smaller lake-level variations than Lake Naskaupi (~30 m variation for Lake McLean and ~60 m for Lake Naskaupi). Lake McLean was also not as extensive or deep as Lake Naskaupi and, as a result, has less well developed shorelines (Barnett, 1967).

In the southern part of the study area, Low (1896) described terraces along the shores of Lake Michikamau (western half of the Smallwood Reservoir), boulder-strewn raised shorelines, and flat-topped islands, all influenced by an unnamed postglacial ice-dammed lake occupying this region. Follow-up work by Tanner (1947) suggested that an ice dam was needed to the south of (then) Lake Michikamau for this lake to develop. Ives (1960b) and Peterson (1965) both recognized these shorelines south of the drainage divide, near the eastern arm of the Smallwood Reservoir and, given the limited data available, concluded they were most likely ice-pushed ramparts. This region was subsequently flooded to create the Smallwood Reservoir with the construction of the Churchill Falls hydroelectric dam in 1974, resulting in the submergence of many of these shorelines.

These glacial lakes are critically important in constraining ice-margin retreat and provide important controls on the overall deglacial patterns of the Quebec–Labrador sector of the LIS. This is exemplified by Clark et al. (2000), who used glacial lakes McLean and Naskaupi, along with other ice-marginal lakes, to constrain ice-margin-retreat patterns, although the timing of many of these lakes remains poorly defined. The lack of organic-rich lake sediments commonly used for ^{14}C dating within the interior of the Quebec–Labrador region and the shortage of well developed glaciolacustrine shorelines suitable for optical dating have made constraining the ages of these glacial lakes difficult.

More recently, cosmogenic ^{10}Be surface-exposure dating has improved understanding of the timing and pattern of ice-margin retreat for the Quebec–Labrador sector (Fig. 4; Clark et al., 2003; Carlson et al., 2008; Ullman et al., 2015, 2016). Collectively, these investigations indicated the region west of

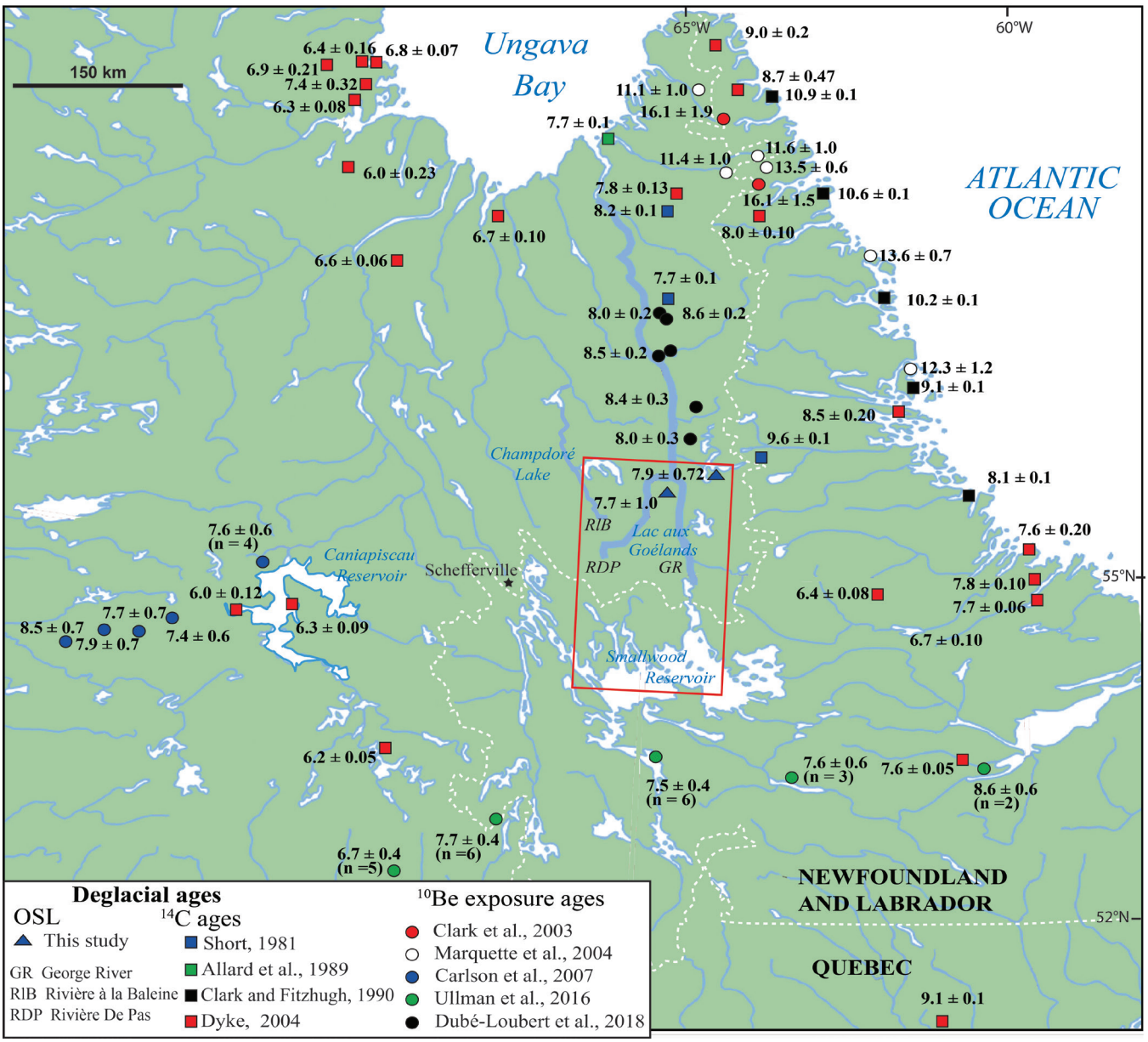

Figure 4. Distribution of previously reported deglacial ages and location of the study area (red box). Deglacial ages are reported in thousands of calibrated years before present (ka cal BP).

the Caniapiscau Reservoir was ice-free by 8.2 ± 0.5 ka and the region south of the Churchill River was ice-free no later than 6.7 ± 0.4 ka, indicating a rapid retreat of the ice margin. North of the study area, ^{10}Be exposure ages of imbricated boulders deposited along raised shorelines and related to the catastrophic drainage of Lake Naskaupi during N2' indicated that the lake at least partially drained around 8.3 ± 0.3 ka (Dubé-Loubert et al., 2018). Dyke (2004) estimated the entire sequence encompassing both Lake Naskaupi and Lake McLean to have occurred between 8.5 and 7.5 ka. However, there are no age constraints for shorelines at the southern extent of Lake Naskaupi (although assumed to have occurred during N2') and no age constraints are available for Lake McLean or glacial lakes in the Smallwood Reservoir area.

Surficial mapping

Douglas and Drummond (1955) created the first small-scale glacial landform map of the Labrador Peninsula through aerial photograph interpretation and field observations. Later work resulted in surficial geology maps of the study area being published at the scales of 1:1 000 000 and 1:5 000 000 (Klassen et al., 1992; Fulton, 1995). More local-scale surficial maps were completed for the surrounding area, with some preliminary surficial maps of the Labrador portion of the study area (Klassen and Paradis, 1990). Ives (1956) brought attention to 'rippled till' west of the study area and discussed the geomorphological relationship of the till with the numerous eskers in the area, proposing a

possible link between the two landform systems. However, follow-up work by Cowan (1967) indicated no relationship between the ribbed moraine (rippled till) and eskers or esker fans, based on field investigations carried out 60 km south of Schefferville. Cowan (1967) concluded that the ribbed till was formed by overriding ice bulldozing material until it accumulated and provided enough resistance to the ice, at which point the ice overrode the material and continued to advance, repeating the process. Jansson et al. (2003) and Jansson (2005) mapped a small part of the study area, as well as a region to the west and northwest of the study area, in more detail and indicated that the region had a much more complex glacial history than previously reported. The surrounding surficial maps did identify important landforms and striation trends for use in ice-flow reconstructions but did not cover the entire study area and lacked detailed separation of surficial units required for modern ice-sheet-modelling studies (e.g. Gowan et al., 2019).

Till geochemical and indicator-mineral dispersal patterns

Klassen and Thompson (1993) conducted an extensive till geochemical survey in western Labrador and parts of east-central Quebec, including the current study area. They identified multiple glacial dispersal patterns formed by early ice-flow phases and modified during later ice-flow phases, creating different footprints based on their geographic location. Along the Quebec–Labrador border, near what would have been the interior of the Quebec–Labrador sector, the dispersal of iron-formation clasts during multiple ice-flow phases in various directions from their source created an ameboid dispersal pattern (grey scale in Fig. 5). However, toward the coast, dispersal patterns become more linear (e.g. Red Wine complex (yellow fan in Fig. 5) and Flowers River igneous suite (green fan in Fig. 5)) as the result of a single or several ice-flow phases in a relatively uniform regional direction. Although the dispersal patterns in Klassen and Thompson (1993) reflect the regional ice-flow phases from that study, the sample survey was limited in extent (i.e. did not cover the full extent of the iron-formation-clast dispersal) and in analytical techniques (i.e. did not use modern total-digestion geochemical analysis). Additionally, the dispersal of iron-formation clasts was based on a qualitative assessment of whether erratics were absent, rare, present, common, or abundant. Follow-up work by Klassen and Knight (1995) used inductively coupled plasma–atomic emission spectrometry and instrumental neutron activation analysis to reanalyze over 2000 till samples collected across Quebec and Labrador. Through this follow-up work, glacial dispersal patterns were identified from till-matrix geochemistry similar to those determined from erratic boulders, albeit with much shorter dispersal distances (e.g. Pb sourced from the Labrador Trough in Klassen and Knight, 1995, Fig. 11).

More recently, Brushett and Amor (2013) identified distribution patterns of elevated chromite-grain abundances (3–6 grains) in regional esker samples in the southwestern part of the study area, which indicated east-southeast transport from a source located somewhere within the Labrador Trough, and elevated abundances of pyrite grains (6–50 grains). Additionally, a few gold grains were identified in samples collected from eskers that extend southeast across the study area. These indicator minerals were thought to have originated from a source within the Labrador Trough or within the Ashuanipi Complex, just west of the Labrador Trough. These prior works on till geochemistry and indicator minerals suggest that glacial dispersal patterns are more complex toward the interior of the Quebec–Labrador sector than in the outer regions, toward the Labrador coast.

Study area

Location and physiography

The study area straddles the provincial border between Quebec and Newfoundland and Labrador, approximately 60 km east of Schefferville, Quebec, and covers over 30 000 km^2 represented on the Wood Lake (NTS 23-I) and Resolution Lake (NTS 23-P) map sheets, between 64° and 66°W longitude and 54° and 56°N latitude (Fig. 1). The largest lakes are the Smallwood Reservoir in the south, Champdoré Lake in the northwest, Lac aux Goélands in the east, and Mistinibi Lake in the northeast. The northern half of the study area is characterized by discontinuous permafrost (50%–90%), often expressed by the presence of frost boils (Smith, 2010). In the southern half, conditions transition to sporadic, discontinuous permafrost (10%–50%). The study area straddles the drainage divide between rivers flowing north/northwest to Ungava Bay and rivers flowing east/southeast to the Atlantic Ocean. The George River drains northward from the divide, past its junction with the Rivière De Pas, then flows through a large river valley (George River valley) into Ungava Bay (Fig. 4). The topography within the study area is typical of Canadian Shield terrain, with undulating low to moderate relief and irregular bedrock knobs. Elevations range from less than 350 m in the George River valley to 704 m on the highest rock knob near the continental drainage divide. Hills and upland regions typically have outcrops with veneers of glacial sediments and are flanked by thicker glacial deposits in the valleys.

The study area lies within the physiographic regions of the Lake Plateau within the James Region and the George Plateau and Whale Lowland divisions of the Davis Region, all of which are within the Canadian Shield physiographic region (Bostock, 2014). Ecologically, the region transitions from the Taiga Shield zone in the north to the Boreal Shield zone in the south (Smith, 2010). The treeline crosses the northern part of the study area, with trees typically growing

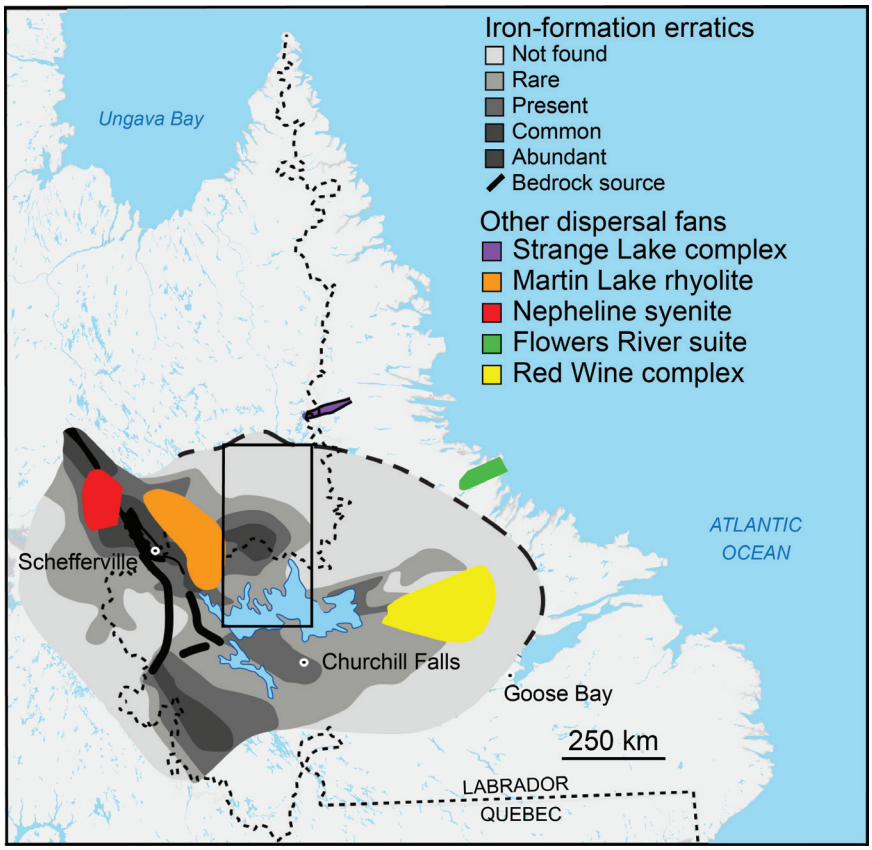

Figure 5. Dispersal patterns identified from erratic boulders by Klassen and Thompson (1993) for iron formation (greyscale) and other unique bedrock lithological units in western Labrador and east-central Quebec (*modified from* Klassen and Thompson, 1993). The study area is outlined in black.

only in the low-lying areas. Moss, lichen, and small shrubs dominate the highland areas, with black spruce and tamarack (larch) constituting much of the lowland forests.

Bedrock geology

The study area is located within the southern Core Zone, a Precambrian lithotectonic terrane of the eastern Canadian Shield (Wardle et al., 2002). The Core Zone is within the southeastern Churchill Province and extends approximately 500 km from the Grenville Orogen, in the south, to Ungava Bay, in the north (Fig. 2). It is bounded to the west by the New Quebec Orogen and to the east by the Torngat Orogen. Two major shear zones transect the region, the Tudor Lake shear zone and the George River shear zone (Fig. 2). These shear zones mark the eastern and western boundaries of the George River block that consists of the De Pas batholith, a large felsic intrusion that forms a prominent upland, and its associated orthogneiss, which bisects the study area (Corrigan et al., 2018). The batholith is a K-feldspar-phyric monzogranite-granodiorite-syenogranite, with more orthopyroxene-rich assemblages in the western half and more hornblende-biotite-rich rocks in the east (Sanborn-Barrie, 2016).

East of the George River block, in the northern half of the study area, is the Mistinibi–Raude Domain (Fig. 2), a complex of supracrustal rocks and plutonic rocks of Neoarchean and Paleoproterozoic age (van der Leeden et al., 1990). The Mistinibi–Raude Domain is capped by the Zeni Lake amphibolite and mylonitic tonalite in the south, which are both bounded to the east by Mesoproterozoic granite. In the southeastern part of the study area, the Core Zone is intruded by Mesoproterozoic plutons and is bounded to the south by the Seal Lake Group (Sanborn-Barrie, 2016) and the Michikamau granite and anorthosite suite of rocks (Fig. 2). In the northwestern part of the study area, the Tudor Lake shear zone marks the boundary between the George River block and the metasedimentary rocks of the Rachel–Laporte Domain to the west. The Rachel–Laporte rocks overlie Churchill Province basement rocks in the northern part of the study area (Fig. 2). South of the Rachel–Laporte Domain, Churchill Province basement rocks are overlain by metavolcanic rocks of the Labrador Trough. The Paleoproterozoic Labrador Trough includes the Kaniapiskau Supergroup that is composed of the Knob Lake Group, which hosts economic iron deposits, in the west and the Doublet Group in the east (Wardle, 1982a, b; Corrigan et al., 2015). A detailed summary of the lithological assemblages within and surrounding the study area can be found in James et al. (1993, 1996), Clark and Wares (2005), Sanborn-Barrie (2016), and Corrigan et al. (2015, 2018).

Surficial geology

Surficial mapping as part of this GEM-2 activity shows the northern part of the study area is characterized by highland clearings covered in till veneer, with abundant small bedrock outcrops and erratics (Rice et al., 2017c, d; Paulen et al., 2020c, d). These uplands are flanked by thicker till blankets in the valleys. Evidence of meltwater reworking and meltwater erosion is also abundant in the north and includes glaciofluvial deposits, a few eskers, kames, and lateral meltwater channels. In the southern half of the study area, organic deposits are much more abundant in the low-lying areas and the esker network is denser as well as more continuous, with only rare meltwater channels (Paulen et al., 2017, 2019a, b). Wave-washed bedrock, winnowed till deposits, and beach sediments occur in areas inundated by glacial lakes Naskaupi, McLean, and Low (*see* 'Deglacial chronology' section below).

METHODS

Field methods

Ice-flow measurements

As part of surficial mapping activities, ice-flow directions were determined by measuring streamlined glacial landforms (e.g. crag-and-tails, drumlins, and large-scale glacial lineations) from both satellite-imagery and aerial-photograph interpretation. Landsat 8 satellite-image mosaics were coupled with the highest resolution data available, a hillshaded digital elevation model (DEM from 30 m resolution Shuttle Radar Topography Mission data), following procedures outlined in Clark et al. (2000) and Stokes and Clark (2001). The DEM was coupled with regional bedrock and aeromagnetic maps to ensure the mapped landforms were not bedrock features. During fieldwork conducted between 2014 and 2016, outcrop-scale ice-flow indicators (e.g. striations, grooves, rat tails, and mini crag-and-tails; Fig. 6) were measured to further clarify the direction of ice flow. The directions of striations and grooves were determined from the shape of the outcrops, including plucking directions. Where multiple sets of ice-flow indicators were identified, relative ages were determined through the examination of older ice-flow indicators in protected lee-side positions on bedrock outcrops (e.g. Veillette and Roy, 1995; McMartin and Paulen, 2009). Once a relative ice-flow chronology was established from outcrop-scale indicators, it was compared to the surrounding landform record to derive more regional-scale flow sets and chronology. Because glaciated terrains are typically fragmented within inner regions of ice sheets (e.g. Gauthier et al., 2019), ice-flow indicator patterns (both landform flow sets and outcrop-scale records) were analyzed across the study area to determine whether disjointed zones with internally coherent records could be identified. This is an important step in the identification and characterization of different palimpsest glacial footprints (e.g. Kleman and Glasser, 2007). In this conceptual model, unmodified older ice-flow indicators are preserved due to a shift from warm-based active ice to cold-based, nonerosive ice. Typically, these relict, unmodified terrains are identified next to an area where they are variably overprinted by later ice-flow phases. Therefore, when ice-flow measurements were conducted, several inherent assumptions were made, including the assumption that subparallel ice-flow indicators on any given polished surface were formed contemporaneously during a single ice-flow phase.

Till-sample collection and analysis

Till samples were collected across the study area for matrix geochemistry, indicator minerals and clast lithology analysis.. Till was sampled at a spacing of approximately 8 to 12 km, using protocols established by GSC scientists (McClenaghan et al., 2013, 2020; Plouffe et al., 2013). The sediment targeted for sampling was determined to be subglacial till, based on its poorly sorted nature, the abundance of striated and faceted clasts within the sediment, and the high degree of compaction. Till samples were collected from hand-dug pits in frost boils or in soil profiles where the C-horizon (unoxidized) till was targeted. During sample collection, larger pebbles (>64 mm) were removed by hand to minimize the sample weight. At each sample location (n = 306 sites), a sample weighing approximately 3 kg was collected for till-matrix geochemistry analysis. At 259 of those locations, an additional sample weighing roughly 10 to 15 kg was collected for indicator-mineral recovery and clast (>2 mm) separation. Field data for collected samples are summarized in Rice et al. (2020a).

For this study, 306 samples collected in 2014, 2015, and 2016 were submitted for till-matrix geochemical analysis in addition to 30 archived GSC samples collected in 1986 and 1987 by Klassen and Thompson (1993). Additionally, 257 samples were submitted for indicator-mineral analysis and 256 samples underwent clast-lithology classification.

Figure 6. Examples of outcrop-scale ice-flow indicators: **a)** mini crag-and-tail (photograph by J.M. Rice; NRCan photo 2020-942); **b)** and **c)** double stoss-and-lee outcrops formed during near complete ice-flow reversals (photograph by J.M. Rice; NRCan photos 2020-943 and -944); **d)** fine polish (i.e. shallow striations) on outcrop indicative of late glacial ice-flow phase (flow 5), with older, deeper grooves parallel to pen tip (flow 4) (photograph by R.C. Paulen; NRCan photo 2020-945); **e)** lee-side preservation of older flow (flow 2) from subsequent ice-flow phase (flow 5), with a bevelled edge indicating the limit of preservation (photograph by J.M. Rice; NRCan photo 2020-946).

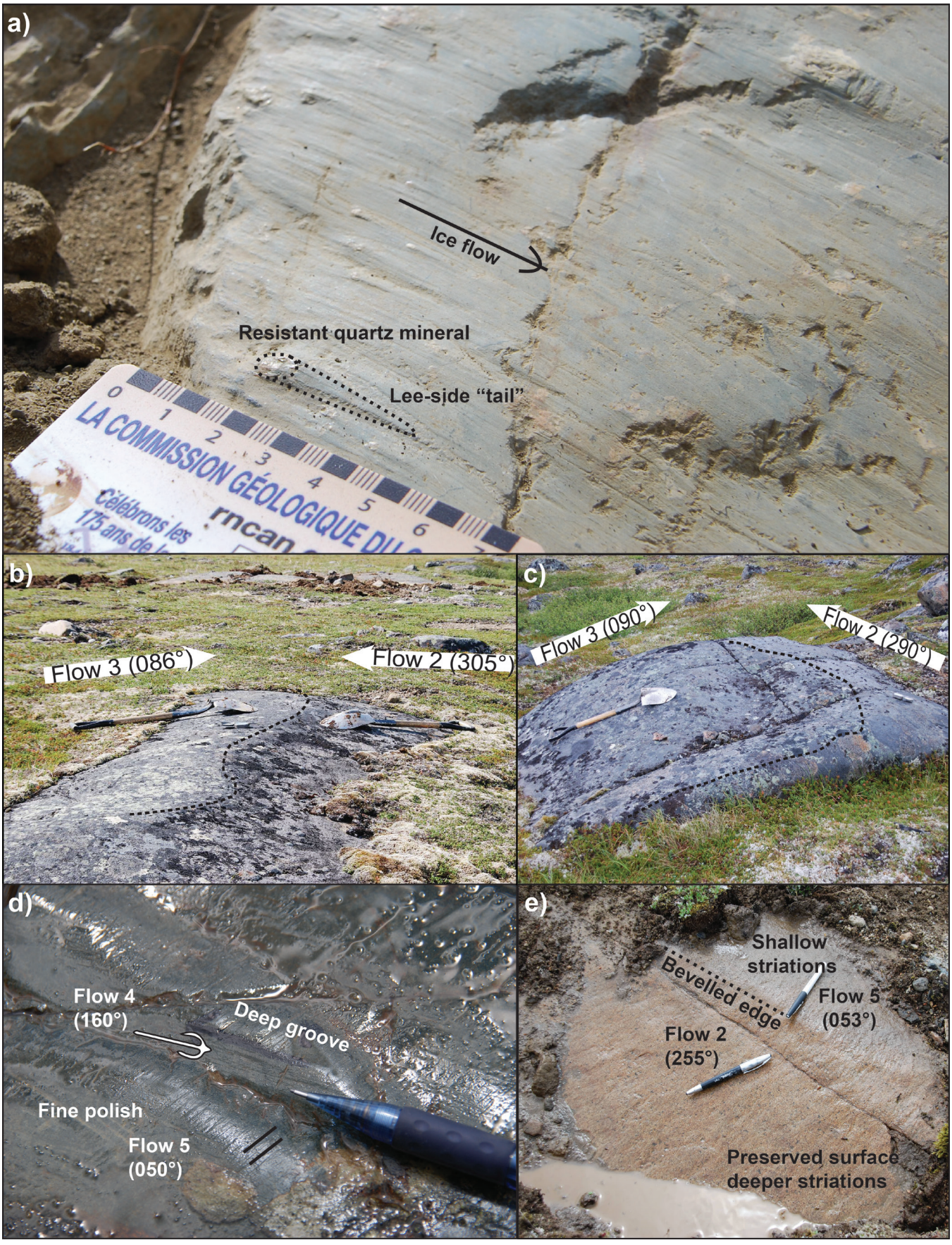
a)
Ice flow
Resistant quartz mineral
Lee-side "tail"
LA COMMISSION GÉOLOGIQUE
b)
Flow 3 (086°)
Flow 2 (305°)
c)
Flow 3 (090°)
Flow 2 (290°)
d)
Flow 4
(160°)
Deep groove
Fine polish
Flow 5
(050°)
e)
Shallow
striations
Bevelled edge
Flow 5
(053°)
Flow 2
(255°)
Preserved surface
deeper striations

Detailed descriptions of the geochemical methodologies, including quality-assurance and quality-control methods, are reported in McClenaghan et al. (2016a) and Rice et al. (2017a). Similarly, sample preparation and analysis for indicator minerals are reported in McClenaghan et al. (2016b, 2017) and Rice et al. (2017b). Detailed methodology for clast-lithology classification is reported in Rice et al. (2017b, 2020b). For this publication, selected indicator-mineral and geochemical results are presented to support the proposed ice-flow reconstruction. The full results of these analyses and a complete list of all published reports from this research program, including published surficial maps, are given in Appendix A.

Geochronological sampling

To constrain the timing of deglaciation within the study area and better understand the paleoglaciological evolution of the Quebec–Labrador sector during ice-sheet collapse, geochronological samples were collected. Two types of geochronological assessments were utilized in this investigation: optically stimulated luminescence (OSL) dating and cosmogenic ^{10}Be surface-exposure age determination. The use of OSL dating to approximate the timing of glacial-lake beach formation has been conducted successfully in other glaciated regions (e.g. Lepper et al., 2013; Hickin et al., 2015). Samples were collected from coarse- to fine-grained sand from the beach ridges of the glacial lakes identified within the study area. For this study, OSL analysis was conducted on feldspar grains, as the quartz grains lacked the 'fast acting component' required for accurate analysis (for details on methods *see* Rice et al., 2019).

Samples of glacially eroded bedrock and glacial erratics were also collected for ^{10}Be exposure dating. At nine sites, a single bedrock sample was collected from elevated, windswept outcrops from lithological units with high (>35%) quartz content. At two of the bedrock-sample sites, erratic boulders were also sampled (15-PTA-081E and 15-PTA-077E). Boulders were selected for sampling on the basis of their quartz content (>35%), size (>1 m^3), stability (no evidence of postdepositional movement), and absence of topographic shielding. Ages were calculated using the online exposure-age calculator (v.3 of the method is available at http://hess.ess.Washington.edu) using the Baffin Bay ^{10}Be production rate (Young et al., 2013) and the nuclide- and time-dependent scaling scheme (Lifton et al., 2014). All ^{10}Be results reported in this study are treated as 'apparent ages' due to the potentially added uncertainty caused by cosmogenic-nuclide inheritance (e.g. Rice et al., 2019). To determine the rate of ice-margin retreat, ^{10}Be samples were collected along an east to west transect parallel to a previously inferred ice-margin-retreat direction (Dyke, 2004). An additional bedrock sample was also collected in the southern half of the area (16-PTA-114B) to assess if deglacial ages were similar to those in the north. All ages reported for ^{10}Be exposure dating and OSL are reported as years before measurement in thousands of years (ka). The ^{10}Be ages are reported at 1σ analytical error and OSL ages are reported at 2σ analytical error, as is standard for each analytical process (Aitken, 1998; Dunai, 2010).

RESULTS AND INTERPRETATIONS

Relative ice-flow chronology

Streamlined-landform mapping identified 1455 crag-and-tails and 1322 drumlinoid ridges across the study area (Fig. 7). Additionally, 403 outcrop-scale ice-flow indicators were measured at 247 locations. Through the mapping of landforms and measurement of striations, regional flow sets were identified and their relative age established; they were then grouped into five ice-flow phases, which are summarized below.

Flow 1

The earliest ice-flow phase identified was to the northeast. This phase is most evident in flow sets in the northeast of the study area (Fig. 7, 8), but it is also correlated with the oldest striations observed elsewhere in the study area (Fig. 8). Flow 1 was remarkably uniform in direction, with only slight deviations in measured striae azimuths (Fig. 8). The lack of striation evidence of this ice-flow phase in the west-central part of the study area is likely due to subsequent erosion of bedrock by later ice-flow phases. The wide distribution of these relatively uniform ice-flow indicators suggests that this phase was warm-based and erosive over much of the study area. Flow 1 was the oldest ice flow at every location except for three sites (15-PTA-147 (345°), 16-PTA-171 (311°), and 16-PTA-154 (350°)), where an even older flow to the north-northeast was noted.

Flow 1 from this study is equivalent to event I of Klassen and Thompson (1993). This ice-flow phase has been identified as one of the oldest phases in the striation record across central Quebec and western Labrador and supports the hypothesis that it could have originated somewhere in the Laurentian Highlands (Klassen and Thompson, 1993; Veillette et al., 1999; Parent, this volume). The absolute age and duration of this phase are unknown, but it has been attributed to the LGM and early deglaciation of the larger Quebec–Labrador sector, when the ice margins were offshore (Dyke and Prest, 1987). No evidence of nonglacial intertill units was observed in the study area, nor was there evidence of ferromanganese staining on any observed outcrops. In contrast to Veillette et al. (1999), who worked within the lowlands of the Caniapiscau Reservoir, the striation observations recorded during this study were made largely on upland areas that could be accessed only by helicopter.

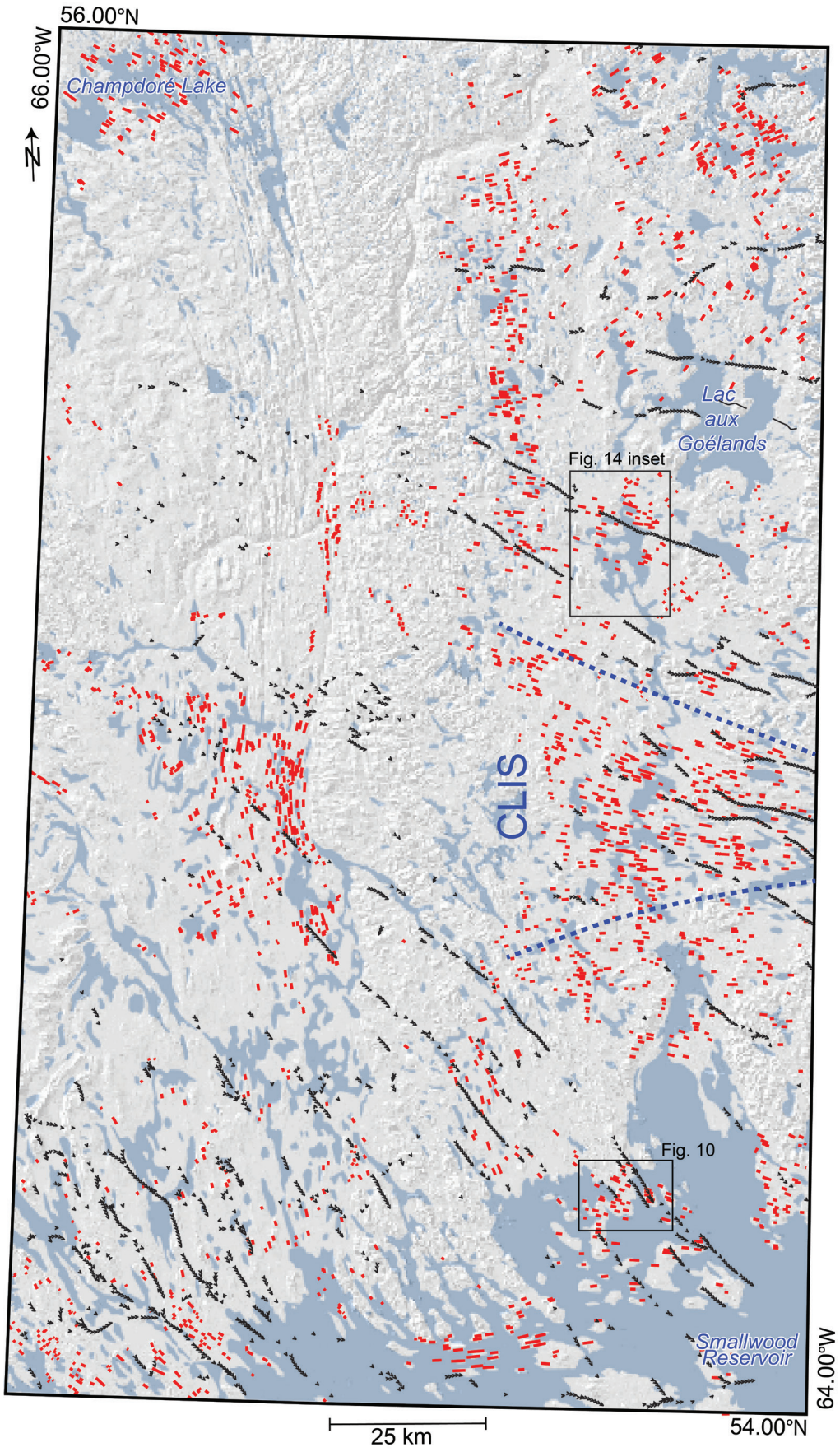

Figure 7. Distribution of elongated subglacial landforms (red lines) and eskers (black lines) across the study area. The Cabot Lake ice stream (CLIS) has been outlined with blue dashed lines (*adapted from* Rice et al., 2017c, d; Paulen et al., 2017, 2019a, b, 2020c, d; Campbell et al., 2018). The black boxes show the locations of Figures 10 and 14.

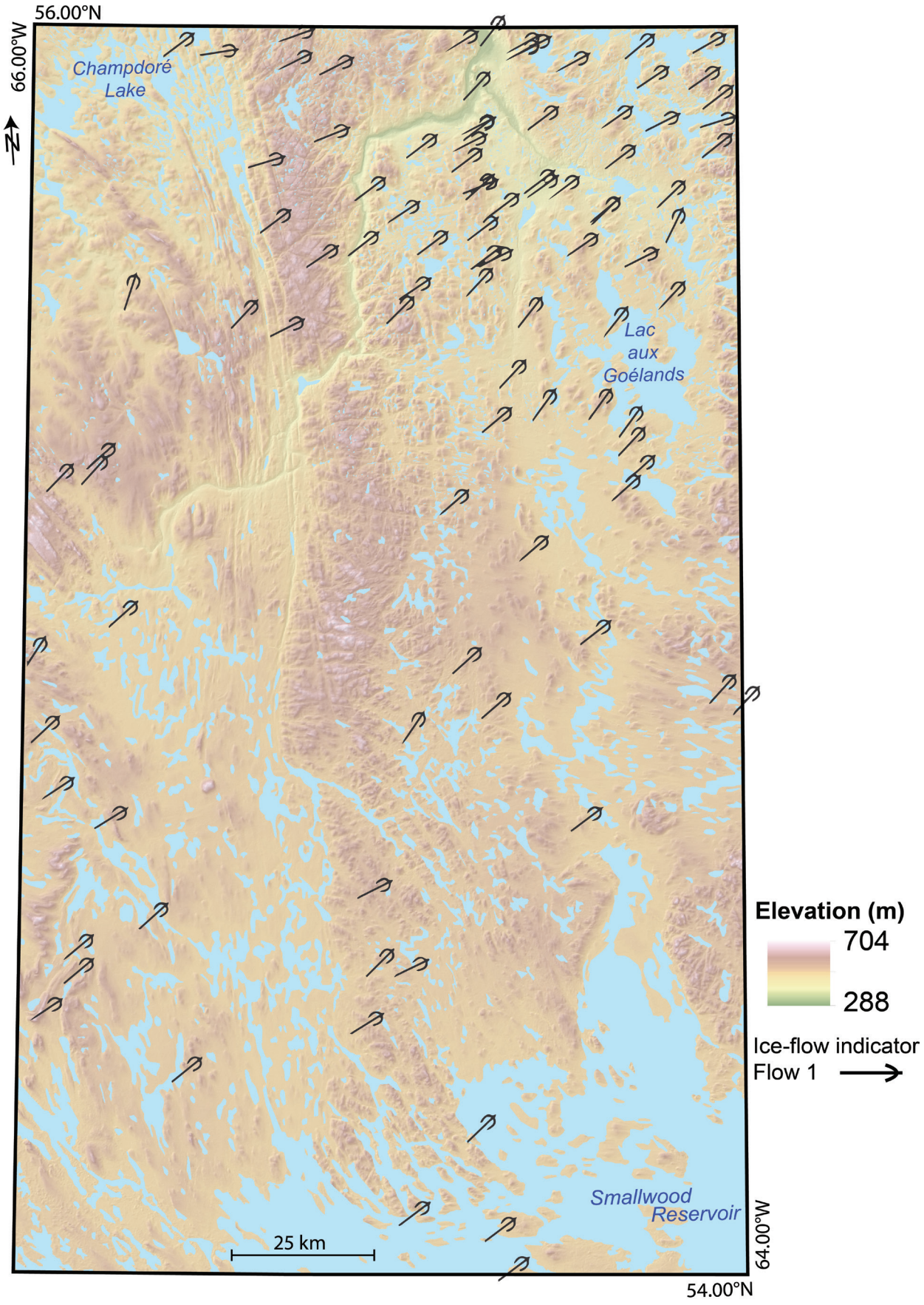
56.00°N
66.00°W
N
Champdoré Lake
Lac aux Goélands
Smallwood Reservoir
25 km
64.00°W
54.00°N
Elevation (m)
704
288
Ice-flow indicator
Flow 1

Figure 8. Outcrop-scale ice-flow indicators associated with flow 1, indicating a relatively uniform flow direction to the northeast across almost the entire study area. In the northeastern corner of the map, flow 3 striations follow a similar azimuth and are therefore difficult to differentiate from flow 1 (*see* Rice et al., 2020d).

Flow 2

The ice-flow direction and subglacial conditions changed drastically after flow 1, as indicated by the degree of preservation of flow 1 features in the northeastern part of the study area and by strong overprinting in the northwest by northwest flow 2 indicators (Fig. 7, 9). This suggests a change from broad, warm-based conditions to more regionally cold-based conditions, except for restricted regions of actively sliding ice mainly in the northwest (e.g. Rice et al., 2020d). Flow 2 overprints flow 1 indicators at six locations and is overprinted by later ice-flow indicators (flow 3) at eight locations, which observations were used to determine its relative chronology. Flow 2 striations are oriented more toward the west in the central part of the study area, where landforms are noticeably absent (Fig. 7). In the central highlands, where evidence of flow 2 remains only on striated bedrock surfaces, either there was not enough sediment to produce landforms or subglacial conditions were not conducive to producing landforms (i.e. the highlands were too close to the divide to form landforms). The hypothesis proposing that an ice divide occupied the northeastern part of the study area is supported by the preservation of landforms associated with flow 1 east and southeast of the flow 2 'footprint' and by old southeast-trending landforms occurring in the southeastern part of the study area (Fig. 7). Although no striation evidence of flow 2 was identified in the southeast, the southeast-trending landforms are overprinted by more easterly flow 3 landforms and consequently must have formed prior to flow 3 (Fig. 10), which suggests that ice flowed in nearly opposite directions from an ice divide located across the study area (Fig. 9) or as the ice divide migrated from east to west.

Flow 2 is similar in orientation to event III of Klassen and Thompson (1993) and the northwest ice-flow phase of Veillette et al. (1999), but the relative chronology presented here differs from that of those authors in that flow 2 from this study occurred before a major eastward phase (their flow II).). Flow 2 is also similar in orientation to flow set 19 of Clark et al. (2000) and fan D (Fig. 3c) of Jansson et al. (2002), which were suggested to have been formed by ice streaming toward Ungava Bay early on during deglaciation. Jansson et al. (2003) indicated the catchment area of the Ungava Bay ice stream migrated west from its original position on the eastern edge of Ungava Bay. This westward migration could have led to the progressive westward shift of the ice divide across the study area. Alternatively, the ice divide may have shifted as eastward-streaming ice propagated up-flow, forcing the divide west. Overall, this ice-divide migration led to a near complete ice-flow reversal within a portion of the study area, resulting in the third ice-flow phase (flow 3).

Flow 3

Irrespective of what caused the westward migration of the divide, ice began to flow eastward toward the Labrador coast during flow 3 (Fig. 11). Flow 3 outcrop-scale indicators crosscut flow 2 at eight key locations, where they are preserved on the lee sides of flow 3 sculpted bedrock outcrops. At 15 locations flow 3 ice-flow indicators were protected (or preserved) from (during) later ice-flow phases. Flow 3 striations are found most everywhere across the study area and are generally oriented to the east. In the northeast, these striations are oriented more to the east-northeast, whereas in the south, they are oriented slightly more to the east-southeast. Closely spaced, converging streamlined landforms associated with flow 3 form an ice-stream corridor (Cabot Lake ice stream; Paulen et al., 2019a; Rice et al., 2020d) in the east-central part of the study area (blue dashed line on Fig. 7).

Flow 3 is similar in orientation to event II of Klassen and Thompson (1993) and, to a degree, to event V east of the study area (Fig. 3b), as well as to the pre-LGM flow identified in Clarhäll and Jansson (2003) in Figure 3d, but does not align with any of these ice-flow chronologies. Some of the shorter northeast-oriented landforms in the northeastern corner of the study area may also be associated with flow 3 as part of the onset zone of the Kogaluk ice stream just northeast of the study area ('#187' in Margold et al., 2015). These shorter landforms are slightly askew from the larger, northeast-oriented landforms in the northeast that formed during flow 1 (Rice et al., 2020c, Fig. 3). About 250 km to the southeast of the study area, the south-trending Happy Valley–Goose Bay ice stream ('#186' in Margold et al., 2015) was suggested to have been active at approximately 8.9 ka ^{14}C BP (Margold et al., 2018). The similar eastward orientation of the Cabot Lake and Kogaluk ice streams, and

Figure 9. Outcrop-scale ice-flow indicators associated with flow 2 are influenced in the northwest by a drawdown into Ungava Bay to the northwest. A local ice divide (D) was located somewhere across the study area (approximate location indicated on map) to account for landforms related to flow 2 in the Smallwood Reservoir area (Fig. 10) but preservation of the flow 1 landforms in the northeast (Fig. 8).

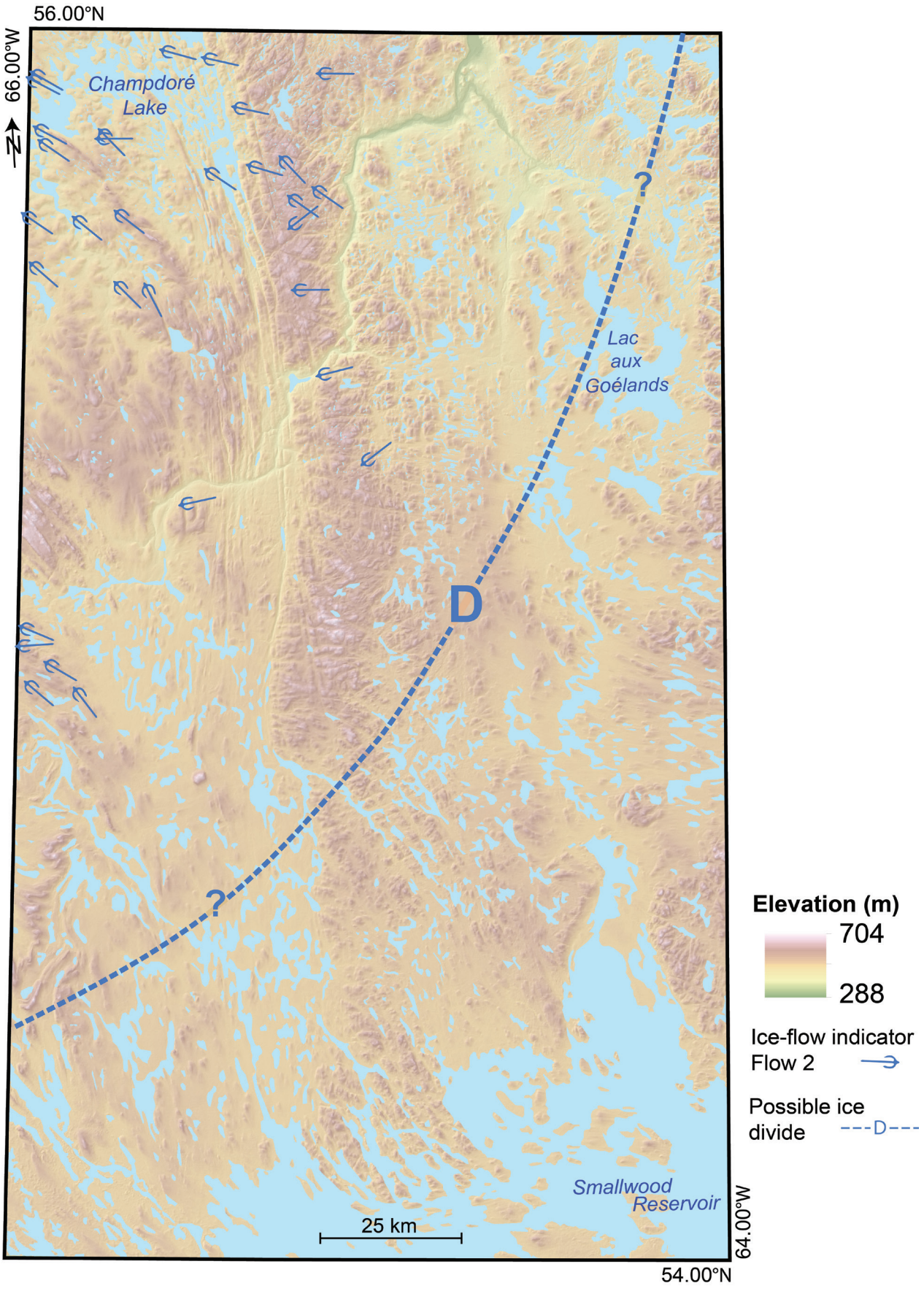
56.00°N
66.00°W
N
Champdoré Lake
Lac aux Goélands
D
?
?
Smallwood Reservoir
25 km
64.00°W
54.00°N
Elevation (m)
704
288
Ice-flow indicator
Flow 2
Possible ice divide
---D---

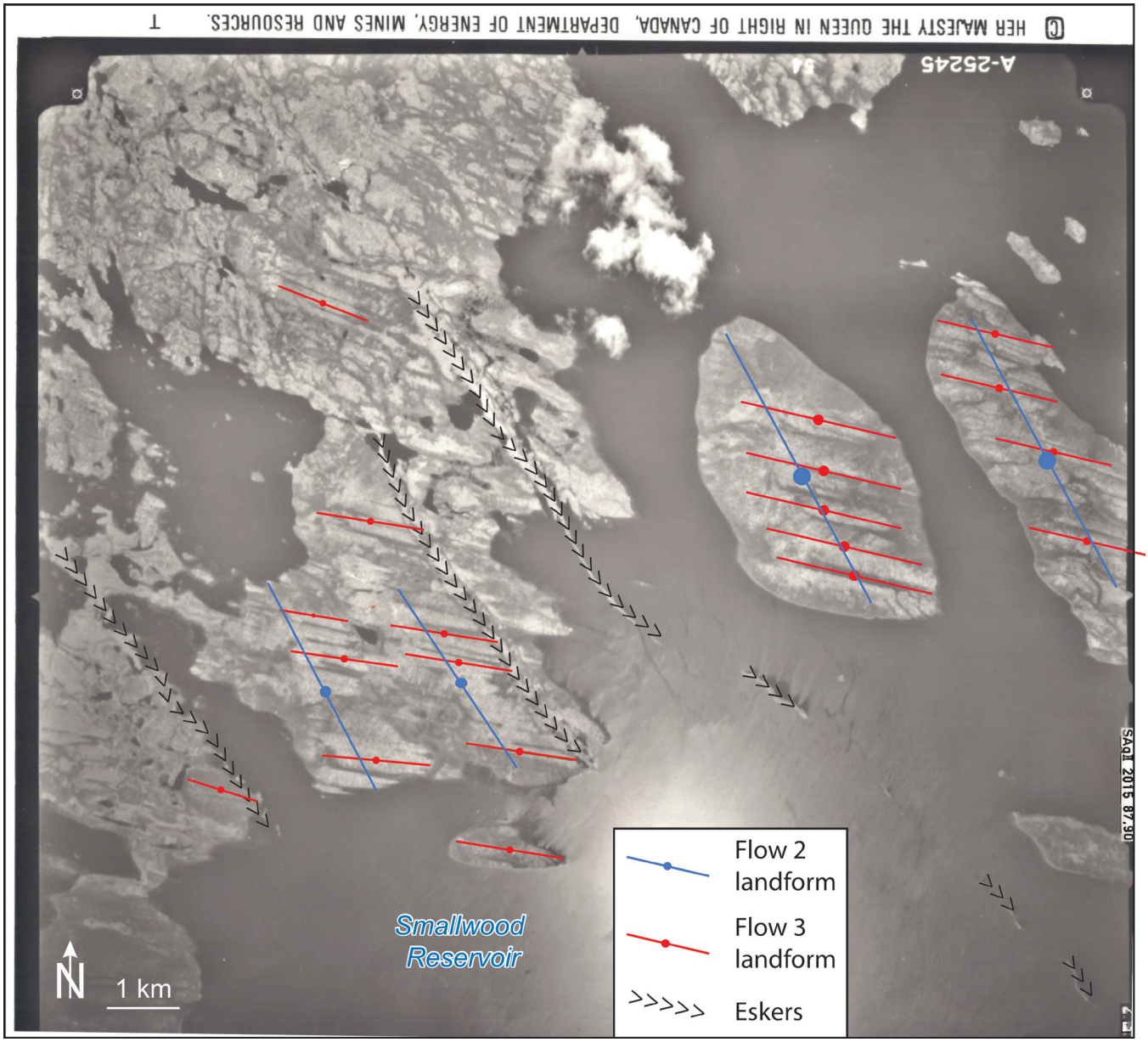

Figure 10. An example of palimpsest landforms in the Smallwood Reservoir, whereby southeast-trending landforms from flow 2 (blue) are overprinted by smaller east-southeast-trending landforms during flow 3 (red). NAPL A25245-54. Note that eskers crosscut the flow 3 landforms and are closer in orientation to flow 4 (*see* Fig. 12).

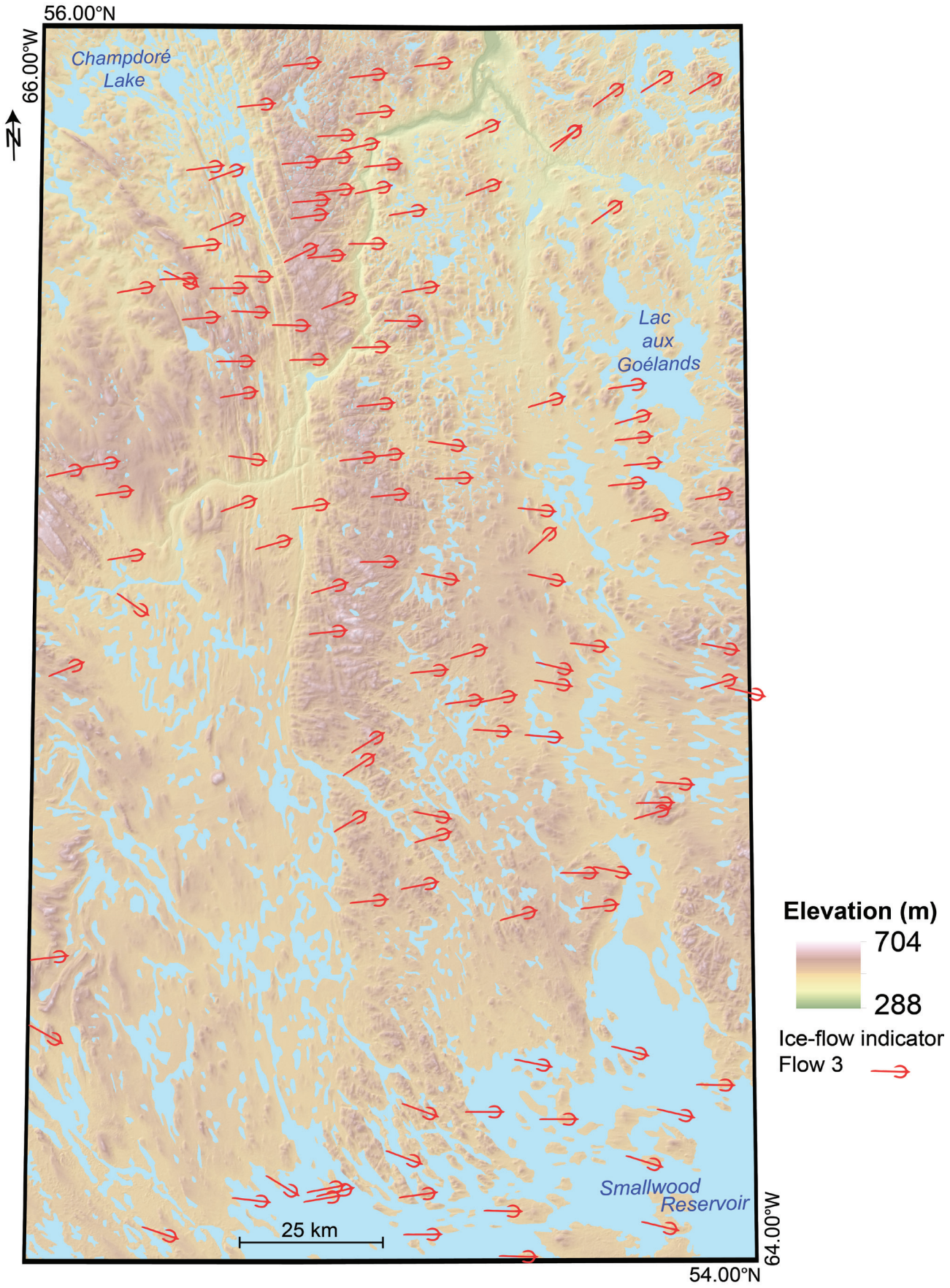
56.00°N
66.00°W
N
Champdoré
Lake
Lac
aux
Goélands
Smallwood
Reservoir
25 km
64.00°W
54.00°N
Elevation (m)
704
288
Ice-flow indicator
Flow 3

Figure 11. Outcrop-scale ice-flow indicators associated with flow 3, showing prevalent flow to the east, which followed the westward migration of the ice divide (then located outside of the study area). Small landforms associated with flow 3 were identified in the northeast of the study area (Rice et al., 2020c); however, the striation record is difficult to discern from flow 1, where crosscutting relationships are not evident (*see* Fig. 8). Where no crosscutting relationship could be established, the striations were assigned to flow 1.

several other ice streams along the Labrador coast, suggests that they were operating around the same time, their location controlled, in part, by the numerous fiords along the Labrador coastline.

Flow 4

Evidence of flow 4 is mainly confined to the southern half of the study area and records a more dynamic south to southeast ice-flow pattern (Fig. 12). Flow 4 overprints flow 3 at 15 locations and is overprinted by flow 5 at 25 locations, which observations were used to determine its relative chronological age. Landforms associated with flow 4 are abundant in the central part of the study area and are confined to the western side of the central upland (Fig. 7). The orientation of glacial landforms and striations suggests that the eastward ice-flow phase (flow 3), gradually shifted to the south (flow 4) into a topographically confined lowland corridor, west of the central uplands, as the ice sheet thinned during deglaciation. Ice flow was then essentially pirated from the central uplands and diverted south, funneled into the Smallwood Reservoir, where it began to flow to the east/southeast (Fig. 12, 13; Paulen et al., 2015, 2017). This type of ice-stream piracy has been identified in the Canadian Prairies (Ross et al., 2009), on Prince of Wales Island (Dyke et al., 1992), and on eastern Baffin Island (Brouard and Lajeunesse, 2019). Eskers mapped in the southern half of the study area are also generally oriented in the same direction as flow 4 (Fig. 7). The parallel orientation of the eskers to flow 4 ice-flow indicators suggests they formed shortly after flow 4 and before final deglaciation of the area, when the ice margin had begun retreating, likely to the northwest (Dyke, 2004; Margold et al., 2018). These findings are consistent with regional interpretations that postulate that the shutdown of eastward ice flows to the Labrador coast (flows 3, 4) was followed by the formation of subglacial meltwater channels and eskers in the region (e.g. Occhietti et al., 2004).

Flow 4 has a similar orientation to event II of Klassen and Thompson (1993) where ice flow is to the south on the west side of the Smallwood Reservoir and to the east on the east side of the Smallwood Reservoir (Fig. 3b) but this was not identified by Jansson et al. (2002) or Clarhäll and Jansson (2003). It should be noted that this flow 4 is not the same flow 4 as previously identified by Rice et al. (2019), which correlates with this study's flow 5 (*see* below).

Flow 5

The youngest ice-flow phase identified within the study area is flow 5 (Fig. 14) and represents late-deglacial flows, when the ice sheet likely thinned and separated into multiple zones of independent ice flows (Ives, 1958; Kirby, 1962; Clark et al., 2000; Rice et al., 2019). With a lowered glacial profile, the formation of ice-flow indicators was largely topographically controlled (i.e. ice predominantly flowing from local highlands to lowlands). Striations formed by this ice-flow phase have a wide range of orientations but do show a preferential orientation to the northeast. Evidence of this ice-flow phase is often identified as a light glacial polish or short, shallow striations on the tops of outcrops, crosscutting older ice-flow indicators (e.g. Fig. 6d). Klassen and Thompson (1993) and Liverman and Vatcher (1992, 1993) also identified topographically controlled late ice flows by a light polish on bedrock outcrops. However, in a small region near Resolution Lake (Fig. 14), streamlined landforms from flow 3 have been reworked by flow 5, forming smaller landforms oriented to the northeast (purple landforms on inset on Fig. 14). These landforms must have occurred following flow 3. They are not of the same age as the flow 1 landforms (black lines), which are larger and have been reworked by flow 3 (red lines) at several sites (*see* inset on Fig. 14). This relative chronology of the landforms correlates well with the striation record observed in nearby uplands.

Deglacial chronology

^{10}Be ages

Ages determined from the most eastern samples (n = 4) range between 6.2 ± 2.1 and 9.8 ± 0.2 ka (Table 1; Fig. 15). Samples collected in the centre of the transect (n = 3) have the largest range in ages, from 7.1 ± 2.9 to 24.0 ± 0.5 ka (Table 1; Fig. 15). Samples collected in the west (n = 4) range in age from 7.9 ± 1.8 to 9.5 ± 0.2 ka (Table 1; Fig. 15). The single sample collected for ^{10}Be age determination in the south

Figure 12. Outcrop-scale ice-flow indicators associated with flow 4. Following the westward migration of the ice divide, ice was deflected south by the topographic highlands in the middle of the study area (De Pas batholith in Fig. 2) and continued to flow southeast into the Smallwood Reservoir.

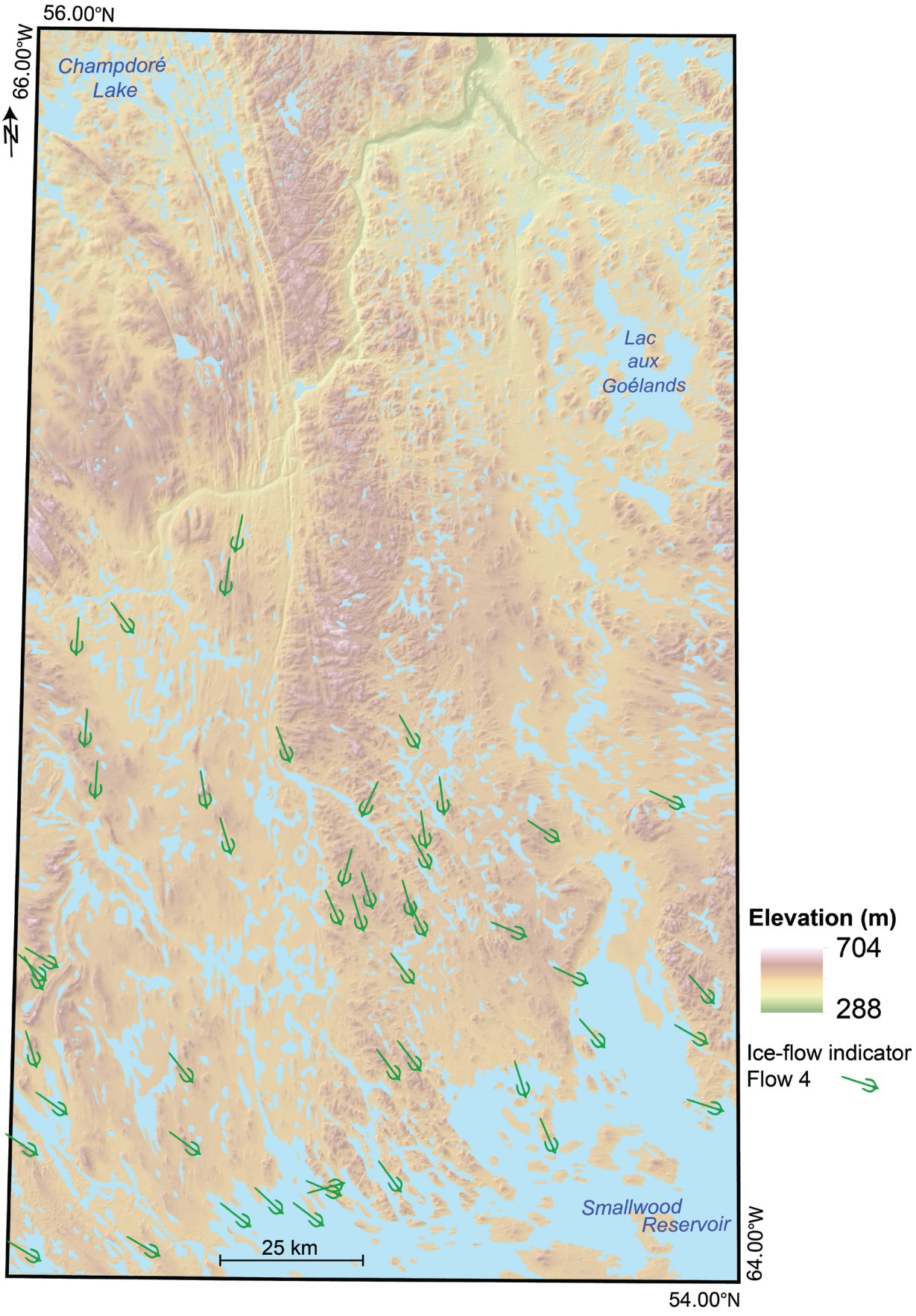
56.00°N
66.00°W
N
Champdoré
Lake
Lac
aux
Goélands
Smallwood
Reservoir
25 km
64.00°W
54.00°N
Elevation (m)
704
288
Ice-flow indicator
Flow 4

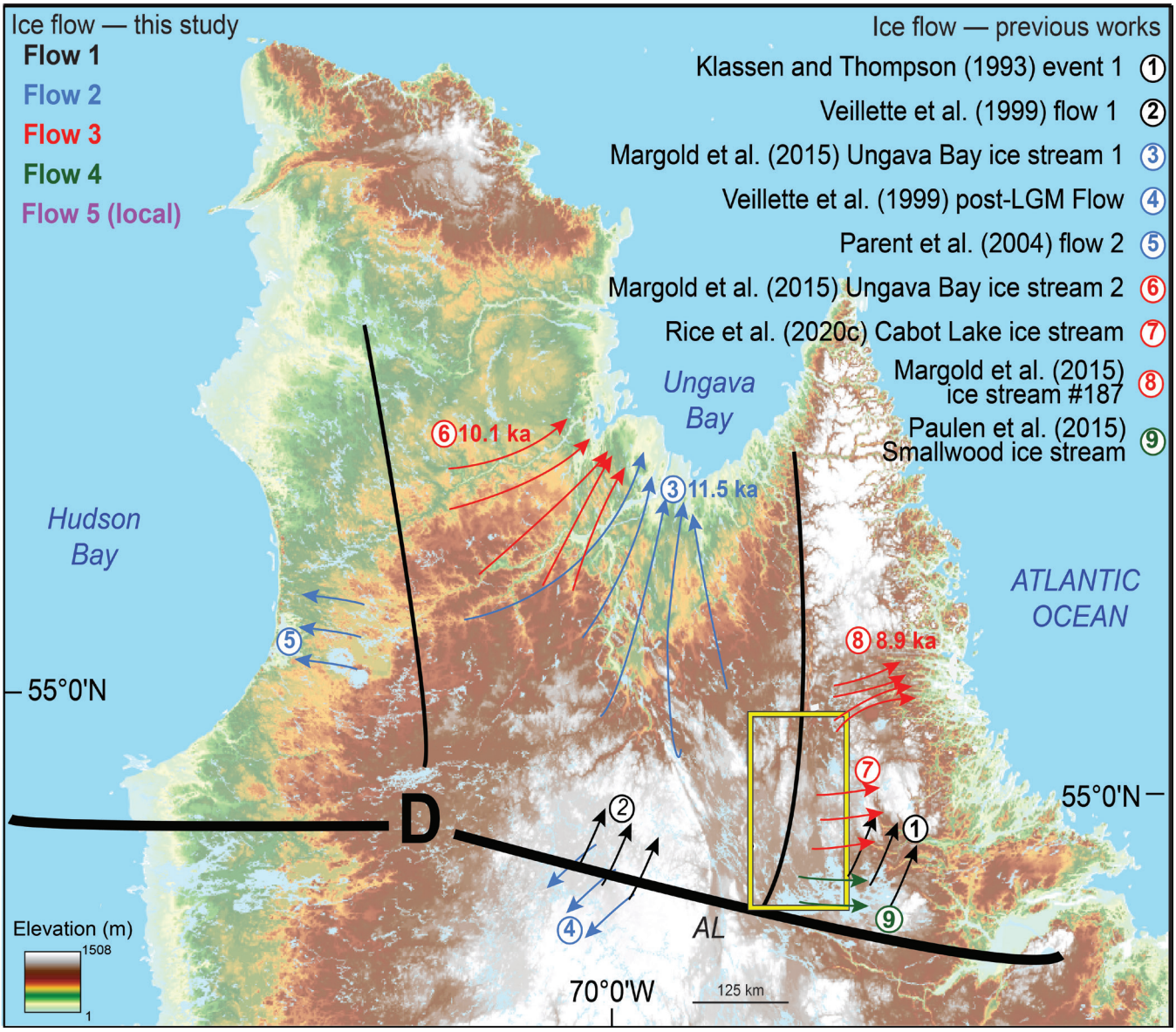

Figure 13. Regional ice-flow phases across Quebec and Labrador, with each ice-flow phase correlated with the ice-flow reconstruction from this study (study area outlined in yellow; flows 1 to 5 in the top left corner). Assigned ages to ice-flow events by Margold et al. (2018) have been indicated next to the identifying number (ages are reported in calibrated years before present (ka BP)). Note that flow 5 is a localized flow and not recorded at the regional scale; therefore, it is not associated to any ice-streaming events. The centre of the Quebec–Labrador dome (D) and Ancestral Labrador Ice Divide (AL) are shown; the major ice-divide locations are represented by thick black lines, and the thinner black lines represent more regional ice divides (Dyke and Prest, 1987). Base map is from Canadian Digital Elevation Model data downloaded from <https://open.canada.ca/data/en/dataset/7f245e4d-76c2-4caa-951a-45d1d2051333>.

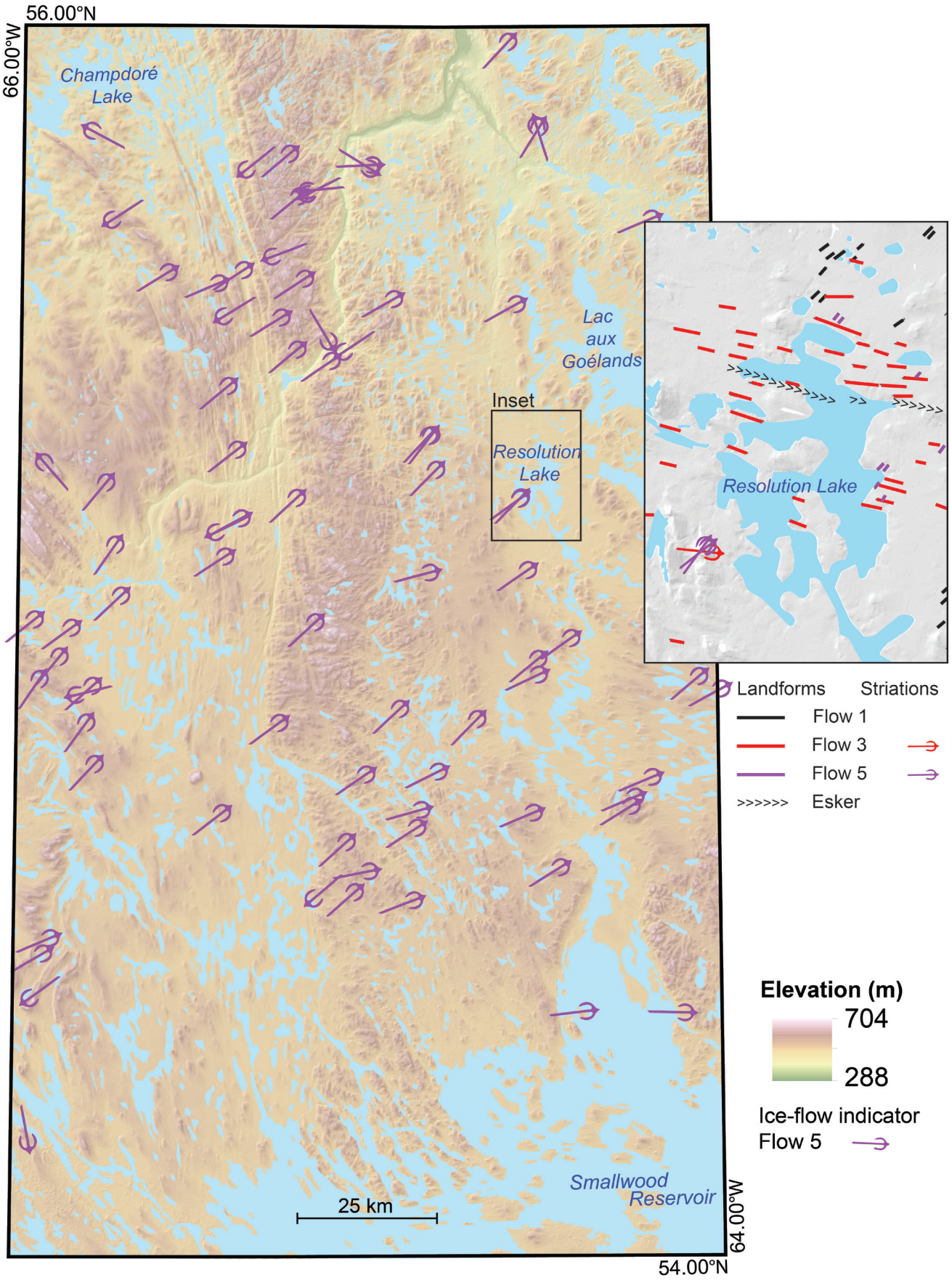
56.00°N
66.00°W
Champdoré Lake
Lac aux Goélands
Inset
Resolution Lake
Resolution Lake
Landforms
Striations
Flow 1
Flow 3
Flow 5
Esker
Elevation (m)
704
288
Ice-flow indicator
Flow 5
Smallwood Reservoir
25 km
64.00°W
54.00°N

Figure 14. Outcrop-scale ice-flow indicators associated with flow 5, when the ice sheet had thinned sufficiently for local topography to become a major factor in controlling local ice-flow directions. As the ice sheet thinned, it split into multiple different smaller ice caps and, in some regions, reworked existing landforms. Landforms and striations illustrated in the inset show flow 1 landforms (black lines) reworked by flow 3 (red lines) in the top of the inset; therefore, they must have been formed prior to flow 3 and are not related to flow 5. Conversely, flow 3 landforms are reworked by flow 5 (purple lines) in the centre of the inset, indicating flow 5 reworked the flow 3 landforms, which were therefore not formed during flow 1. Striations recorded on a local upland show the relative chronology between flow 3 and flow 5.

Table 1. ^{10}Be sample information for bedrock and erratic (E) samples.

Sample	Lat. (°N)	Long. (°W)	Elev. (m a.s.l.)	Corr. elev. (m a.s.l.)[a]	Thick (cm)	Topographic shielding correction	^{10}Be atoms/g	± atoms/g	Thickness scaling factor	Exposure age (a)[b] ± error[c]
East										
15-PTA-058	55.843	64.207	494	433	3.0	1	4.84E+4	1.23E+3	0.976	7 800 ± 200
15-PTA-078	55.821	64.515	517	456	2.5	1	6.28E+4	1.24E+3	0.980	9 800 ± 200
15-PTA-081*	55.810	64.189	559	498	2.0	1	6.10E+4	2.03E+4	0.984	9 200 ± 3 100
15-PTA-081E*	55.810	64.189	559	498	1.5	1	4.13E+4	1.37E+4	0.988	6 200 ± 2 170
Centre										
15-PTA-077*	55.810	65.080	495	434	3.0	1	4.35E+4	1.78E+4	0.976	7 100 ± 2 900[d]
15-PTA-077E	55.810	65.080	495	434	2.0	1	1.03E+5	2.35E+4	0.984	16 700 ± 3 800[d]
16-PTA-070	55.784	65.251	623	562	1.0	1	1.67E+5	3.14E+3	0.992	24 000 ± 500
West										
16-PTA-053	55.867	65.709	517	456	3.0	1	5.36E+4	1.19E+3	0.976	8 500 ± 200
15-PTA083	55.772	65.721	509	448	1.0	1	5.95E+4	1.14E+3	0.992	9 500 ± 200
15-PTA-021*	55.838	65.729	529	468	2.0	1	5.07E+4	1.14E+4	0.984	7 900 ± 1 800
South										
16-PTA-114B	54.181	65.29	565	504	3.5	1	1.06E+5	1.79E+3	0.976	16 454 ± 300[d]

[a]Elevations (elev.) were corrected to isostatic uplift by averaging the uplift from modern elevation in metres above sea level (m a.s.l.) using data from ICE-6G_C(VM5a) (Argus et al., 2014; Peltier et al., 2015)
[b]Be ages reported at 1σ accelerator mass spectrometry uncertainties and calculated using the scaling scheme for spallation of Lal (1991) and Stone (2000)
[c]Error is reported to 1σ of internal uncertainty. Values have been rounded to nearest 10s value.
[d]Outlier samples
*Sample analyzed by Purdue Rare Isotope Measurement Laboratory, West Lafayette, Indiana

Figure 15. Geochronological results from the study area underlain by surficial geology maps (*adapted from* Paulen et al., 2017, 2019a, b, 2020c, d; Rice et al., 2017a, b; Campbell et al., 2018). White dots represent results from bedrock and erratic (E) samples analyzed for cosmogenic ^{10}Be. Yellow dots represent optically stimulated luminescence age on samples of beach sand. Ages are reported in calibrated years before present (ka BP). Several anomalous ages are considered outliers and are not interpreted to reflect deglacial timing.

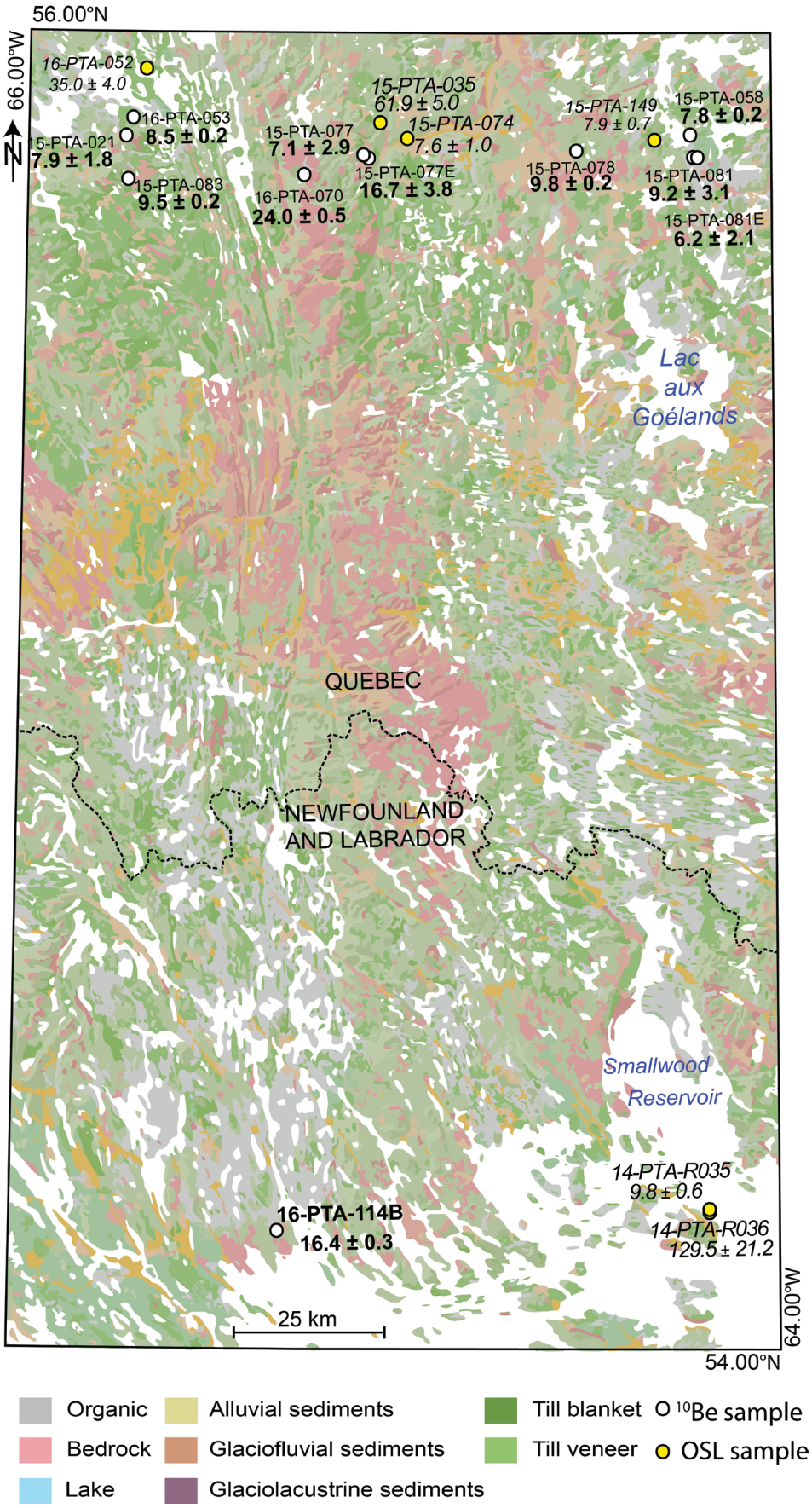
56.00°N
66.00°W
64.00°W
54.00°N
N
16-PTA-052
35.0 ± 4.0
16-PTA-053
8.5 ± 0.2
15-PTA-021
7.9 ± 1.8
15-PTA-083
9.5 ± 0.2
15-PTA-077
7.1 ± 2.9
16-PTA-070
24.0 ± 0.5
15-PTA-035
61.9 ± 5.0
15-PTA-074
7.6 ± 1.0
15-PTA-077E
16.7 ± 3.8
15-PTA-149
7.9 ± 0.7
15-PTA-078
9.8 ± 0.2
15-PTA-058
7.8 ± 0.2
15-PTA-081
9.2 ± 3.1
15-PTA-081E
6.2 ± 2.1
Lac
aux
Goélands
QUEBEC
NEWFOUNLAND
AND LABRADOR
Smallwood
Reservoir
14-PTA-R035
9.8 ± 0.6
14-PTA-R036
129.5 ± 21.2
16-PTA-114B
16.4 ± 0.3
25 km
Organic
Bedrock
Lake
Alluvial sediments
Glaciofluvial sediments
Glaciolacustrine sediments
Till blanket
Till veneer
10Be sample
OSL sample

(16-PTA-114B) has an age of 16.4 ± 0.3 ka, which, along with two samples from the north-central area (16-PTA-070: 24.0 ± 0.5 ka; 15-PTA-077E: 16.7 ± 3.8 ka), are considered to be outliers because they are much older than other samples in the study area and much older than other regional ^{10}Be deglacial ages (Fig. 4; Carlson et al., 2007, 2008; Ullman et al., 2016; Dubé-Loubert et al., 2018). These outliers likely reflect a lower rate of glacial erosion. Typically, at least 2 to 3 m of bedrock material need to be eroded to completely remove preglacial ^{10}Be buildup (Staiger et al., 2006); otherwise, ^{10}Be abundances produce anomalously old ages due to inheritance (*see* Rice et al., 2019).

OSL ages

An OSL sand sample collected from a beach ridge formed by glacial Lake McLean, above the shores of modern-day Champdoré Lake, yielded an age of 35.0 ± 4.0 ka (Table 2; Fig. 15). This anomalously old age likely indicates that the luminescence for feldspar grains was not completely zeroed during deposition (e.g. Fuchs and Owen, 2008). Two OSL samples were also collected from raised shorelines of glacial Lake Naskaupi and another from an outwash terrace associated with a lower phase of Lake Naskaupi. The outwash terrace sample (15-PTA-074; elev. 314 m) represents the lowest and latest stage of Lake Naskaupi, where beaches were not observed and meltwater channels from stagnating ice masses were feeding into the Rivière De Pas valley. Sample 15-PTA-074 was collected from well sorted sand with lower flow-regime sedimentary structures and yielded a fading-corrected age of 7.65 ± 0.99 ka (Table 2). The OSL sample collected from beach sediments at the western edge of Lake Naskaupi (15-PTA-035; 464 m) produced an anomalously old age (61.9 ± 5.02 ka; Table 2). The age from the highest Lake Naskaupi beach (15-PTA-149; 486 m) yielded a fading-corrected age of 7.93 ± 0.72 ka (Table 2) and is thought to be close to the true age of the deposit (Rice et al., 2019).

The two OSL samples from a raised beach formed by a lake in the southeast of the study area (465 m) yielded contrasting optical ages (Table 2). Sample 14-PTA-R036 yielded an anomalously old age of 129.5 ± 21.2 ka, which suggests insufficient bleaching of the grains prior to deposition (e.g. Rice et al., 2019). However, results from a second sample collected from the same section (14-PTA-R035) yielded an age of 9.8 ± 0.6 ka (Paulen et al., 2020a). This OSL age could possibly be as young as 8.6 ka with the analytical uncertainty considered at two standard deviations. If this age is valid, it would require that either the lake basin was ice-free about 1 to 2 ka earlier than what was suggested by previous ice-margin retreat reconstructions (Dyke, 2004; Ullman et al., 2016; Dalton et al., 2020) or this sample was only partially bleached. Given the ages of other beach samples within the study area and regional samples outside the study area (e.g. Dubé-Loubert et al., 2018), an age overestimation is likely.

Table 2. Optically stimulated luminescence (OSL) sample collection data.

Sample ID	Elevation (±5 m a.s.l.)	Depth (cm)	H_2O^a (Δ^w)	K (%)	Rb (ppm)	Th (ppm)	U (ppm)	D_e (CAM) (Gy)	Uncorrected CAM age (ka)	Fading-corrected CAM^b age estimate (ka)^c	Fading-corrected MAM^b age estimate (ka)^c
15-PTA-035	464	100	0.008 8 ± 0.001	2.50 ± 0.13	52.5 ± 2.77	3.00 ± 2.77	0.39 ± 0.08	23.0 ± 4.0	40.0 ± 3.2	61.9 ± 5.02	29.9 ± 3.10
15-PTA-074	314	370	0.185 ± 0.002	1.80 ± 0.1	61.8 ± 3.31	5.50 ± 0.28	2.13 ± 1.69	7.0 ± 1.0	6.13 ± 0.79	7.65 ± 0.99	n/a
15-PTA-149	486	75	0.032 9 ± 0.003	2.40 ± 0.1	108 ± 5.50	5.50 ± 0.28	1.30 ± 0.11	33.0 ± 5.0	6.59 ± 0.60	7.93 ± 0.72	4.59 ± 0.45
14-PTA-R035	464	0.8	0.035 ± 0.010	1.8 ± 0.1	46 ± 4	5.6 ± 0.3	0.4 ± 0.1	28.5 ± 0.7	8.7 ± 1.8	9.8 ± 0.6	n/a
14-PTA-R036	465	1.8	0.035 ± 0.010	2.7 ± 0.1	70 ± 4	3.7 ± 0.2	0.3 ± 0.1	452.9 ± 69.4	114.9 ± 29.2	129.5 ± 21.2	n/a
16-PTA-052	426	140	0.021 ± 0.010	2.9 ± 0.1	80 ± 5	20.6 ± 0.5	1.3 ± 0.1	120.8 ± 10.8	21.6 ± 3.6	35.0 ± 4.0	15.5 ± 2.7 (20.5 ± 3.5)

[a]Water contents are 'as collected' values and are defined as (mass water)/(mass minerals)
[b]Fading corrections were applied using the method of Huntley and Lamothe (2001). Because the natural signal (Ln/Tn) falls in the nonlinear part of the dose-response curves of samples, this correction method may underestimate the true age by ~15%–20% (e.g. Mathewes et al., 2015).
[c]MAM age in brackets excludes two lowest outlying D_e values
Elevation given in metres above sea level (m a.s.l.)
CAM: central age model
MAM: minimum age model

Till-matrix geochemistry

Bedrock lithological units with a distinct geochemical composition that can be recognized in till are limited to the western half of the study area (e.g. metavolcanic units, iron formations). A distinct Cu-dispersal pattern can be observed around the metavolcanic rocks of the Doublet zone, with the highest values located within the zone, decreasing to the northeast, east, and southeast (Fig. 16). Elevated Sb concentrations in the southwestern part of the study area (Fig. 17) reflect the underlying iron formation and associated sedimentary rocks of the Labrador Trough. These are also correlated with elevated Sb concentrations in lake sediments along the entire 800 km length of the Labrador Trough (Amor et al., 2019). Decreasing Sb concentrations are also observed in the northeast, east, and southeast. Base-metal values in till samples reflect the composition of local and proximal (up-ice) mineralized rocks in the Labrador Trough and glacial transport to the northeast, east, and southeast.

Indicator minerals

Goethite, a mineral known to be abundant throughout the Labrador Trough's iron-bearing formations (Neal, 2000), is observed in highest abundances in the western part of the study area, with dispersal to the northeast and east (Fig. 18). Within the centre of the study area, orthopyroxene, which was reported to have elevated concentrations in the western orthogneiss (Sanborn-Barrie, 2016), shows a strong eastward dispersal pattern from the source area (i.e. northeast fanning down to southeast dispersal) and a northwest dispersal pattern in the northwestern part of the study area (Fig. 19).

Clast lithologies

Glacial dispersal patterns identified from bedrock lithological units include the dispersal of iron-formation clasts to the northeast and east from the Labrador Trough bedrock domain (Fig. 20) and the dispersal of felsic intrusive clasts, predominantly sourced from the George River block, to the east and to the northwest in the Champdoré Lake area (Fig. 21). It is difficult to determine if the dispersed iron-formation clasts are the result of northeast or east transport, or both, partially due to the orientation of the source area that extends to the northwest, outside the study area (Fig. 2). The high concentrations of felsic intrusive clasts in the Champdoré Lake area are probably related to a northwest transport, although quartzofeldspathic units in this area are visually identical to those in the De Pas batholith (Corrigan et al., 2018).

DISCUSSION

Ice-flow chronology and glacial dispersal patterns

The glacial history of the study area is characterized by multiple ice-flow phases, major changes in ice-flow directions, and complex glacial dispersal patterns resulting from ice-divide migration (Klassen and Thompson, 1993; Veillette et al., 1999) and related changes in subglacial thermal conditions (Jansson et al., 2002; Clarhäll and Jansson, 2003). The detailed characterization of these ice-flow phases within the inner regions of the Quebec–Labrador sector presented in this study helps resolve some of the contradictions and uncertainties regarding the previously proposed relative ice-flow chronologies and resulting dispersal patterns. Below, the timing of each ice-flow phase within the study area is discussed as a means of more clearly understanding larger scale ice-sheet dynamics. The data presented in this study are used, as well as a detailed analysis of the surficial geological record in the northern part of the study area (Rice et al., 2019, 2020c), to discuss the changing subglacial regimes and their effects on glacial transport in the study area.

Flow 1 likely occurred after the last interglacial (MIS 5e (~123 ka)) as suggested by relatively low ^{10}Be abundances from outcrops within the flow 1 landscape (i.e. limited to no inheritance; Rice et al., 2019). This is also supported by relatively low chemical index of alteration (CIA) values from till-matrix geochemistry samples collected in the northern part of the study area (Rice et al., 2020c). The CIA values in this area (av. 50) are significantly lower than CIA values correlated with regions of sustained cold-based conditions on Baffin Island (i.e. >70; Refsnider and Miller, 2010), suggesting there was sufficient subglacial erosion to remove the preglacial weathering signal in the flow 1 landscape. If flow 1 was from an older glacial event (i.e. pre-MIS 5e), bedrock outcrops with flow 1 evidence should have higher ^{10}Be inheritance and, in nearby till, higher CIA values. This hypothesis is supported by observations of an early northeast ice-flow phase identified in the surrounding regions (i.e. Klassen and Thompson, 1993; Veillette et al., 1999) and the broad evidence of flow 1 across most of the study area, which, taken together, suggests flow 1 was an extensive warm-based ice-flow phase that must have occurred while the Quebec–Labrador dome was quite thick, possibly during the LGM (MIS 2), and was not likely a pre-LGM flow (*cf.* Klassen and Thompson, 1993; Veillette et al., 1999; Jansson et al., 2002; Clarhäll and Jansson, 2003). Glacial dispersal during flow 1 is difficult to evaluate due to reworking and re-entrainment

Figure 16. Proportional-dot map of Cu concentrations in the fraction smaller than 63 µm of till samples analyzed using aqua regia digestion followed by inductively coupled plasma–mass spectrometry (*see* Fig. 2 for bedrock geology legend). The main source area of Cu lies within the Doublet zone.

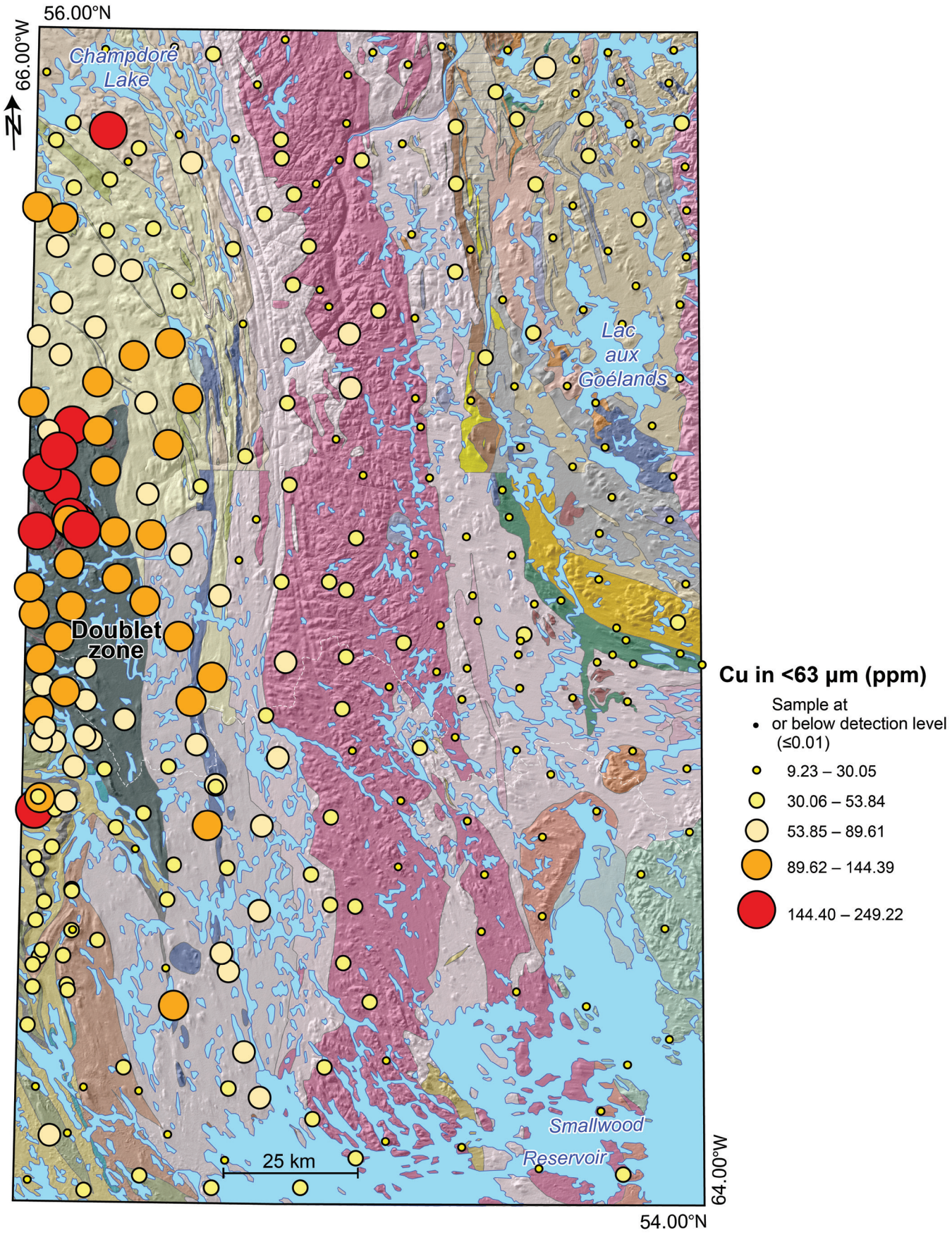
56.00°N
66.00°W
N
Champdoré Lake
Lac aux Goélands
Doublet zone
25 km
Smallwood Reservoir
64.00°W
54.00°N
Cu in <63 µm (ppm)
Sample at or below detection level (≤0.01)
9.23 – 30.05
30.06 – 53.84
53.85 – 89.61
89.62 – 144.39
144.40 – 249.22

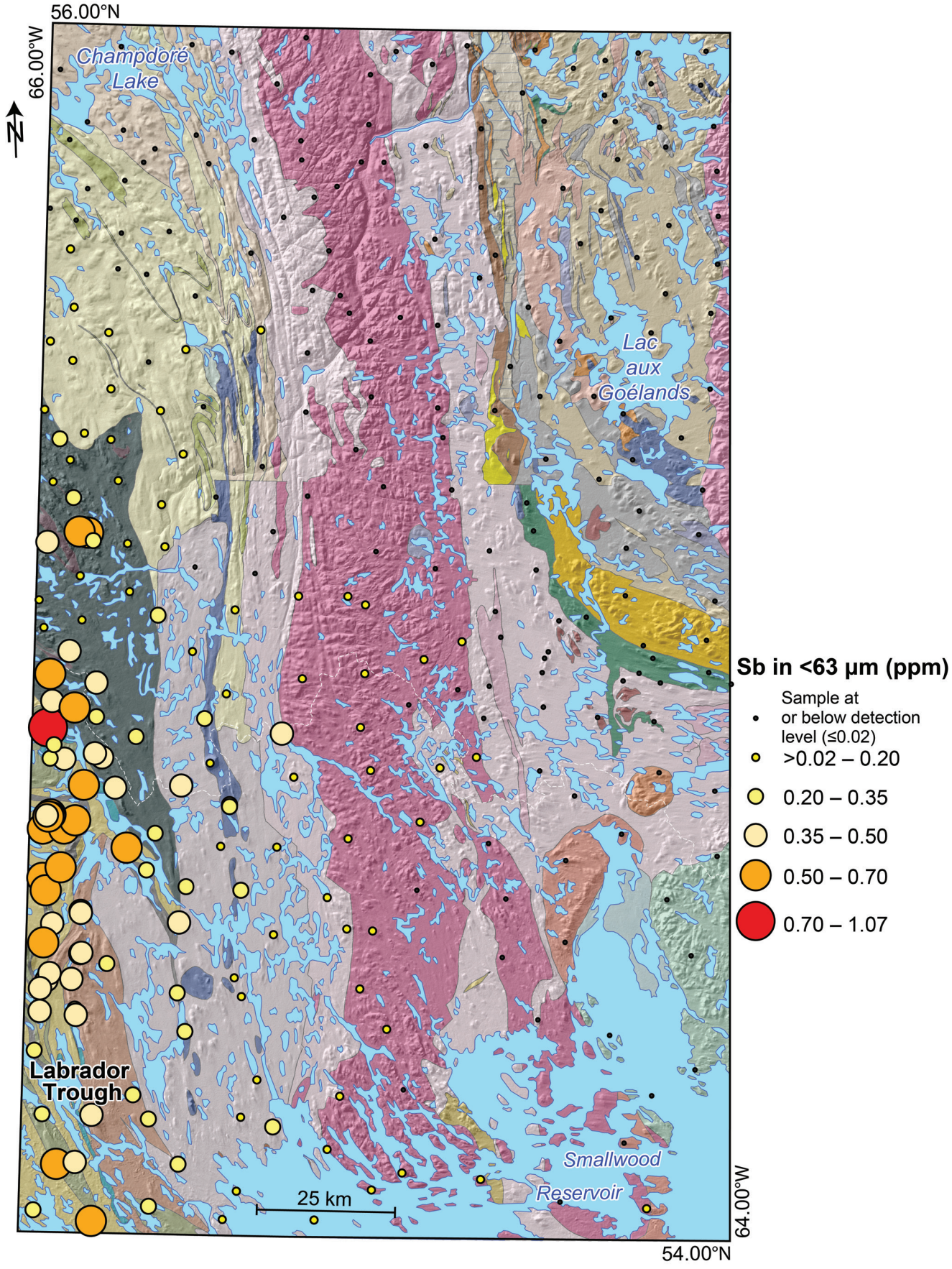
56.00°N
66.00°W
Champdoré Lake
Lac aux Goélands
Labrador Trough
Smallwood Reservoir
25 km
64.00°W
54.00°N
Sb in <63 µm (ppm)
Sample at or below detection level (≤0.02)
>0.02 – 0.20
0.20 – 0.35
0.35 – 0.50
0.50 – 0.70
0.70 – 1.07

Figure 17. Proportional-dot map of Sb concentrations in the fraction smaller than 63 µm of till samples analyzed using aqua regia digestion followed by inductively coupled plasma–mass spectrometry (*see* Fig. 2 for bedrock geology legend). The source areas for Sb are the iron formations of the Labrador Trough.

during subsequent ice-flow phases; however, certain patterns are still discernible. Trace elements, indicator minerals, and clasts that are characteristic of the Labrador Trough (Cu, Sb, goethite, and iron-formation clasts) show evidence of northeast dispersal, with iron-formation clasts having been transported over 75 km from the bedrock source. Klassen and Thompson (1993) attributed northeast dispersal patterns with significant transport distances (up to 100 km from the bedrock source) to their earliest ice-flow phase (event I). The dispersal of iron-formation clasts over such a long distance somewhat conflicts with Rice et al. (2020c), who reported a transition to less erosive conditions in the central uplands (De Pas batholith in Fig. 2), suggesting lower bed mobility and, theoretically, shorter dispersal distances. The development of these large dispersal fans over a low-erosion zone suggests that, although the bedrock geology of the central uplands was more resistant to glacial erosion than other bedrock units, glacial dispersal was not impeded completely, allowing for long distance transport to occur. The mechanisms involved in long glacial transport over a portion of a low-erosion subglacial bed under steady-state glacial conditions remain enigmatic, although they may be related to reduced abrasion over hard beds (Alley et al., 2019) or glacial ripping of large bedrock blocks along bedrock fractures (Hall et al., 2020).

Following flow 1, ice began to flow to the northwest (flow 2), influenced by ice streaming into Ungava Bay. Northwest dispersal patterns of orthopyroxene grains and felsic intrusive clasts provide evidence of northwest glacial transport in the Champdoré Lake area resulting from flow 2. Dispersal evidence to the northwest is limited elsewhere, as there was limited basal sliding occurring near and under a cold-based ice divide somewhere in the northeast of the study area (Fig. 9). Southeast dispersal correlated with flow 2 is more difficult to assess due to the overprinting by later ice-flow phases within the Smallwood Reservoir area (e.g. Fig. 10). Klassen and Thompson (1993) attributed northwest dispersal of the Martin Lake rhyolite (Fig. 5) to their event III toward Ungava Bay (flow 2 in this study). The dispersal pattern of these clasts also has a dispersal component to the southeast (*see* Klassen and Thompson, 1993, Fig. 20), which was identified as the result of ice-divide migration across the bedrock source, similar to the ice-divide migration between flow 2 and flow 3 within the study area.

As the ice divide migrated west, ice began to flow east during flow 3 in a nearly opposite direction to flow 2, at least in the northwestern part of the study area. The activation of the Cabot Lake ice stream in the study area during flow 3 (Paulen et al., 2019a; Rice et al., 2020d) was associated with the early offshore recession of the LIS and interpreted to have occurred contemporaneously with other ice streams flowing toward the Labrador coast (red arrows on Fig. 13). This transition from flow 2 to flow 3 appears to mark the boundary of the eastern arm of the U-shaped unconformity, suggesting the U-shaped boundary reflects changing subglacial thermal conditions, whereby warm-based ice formed northwest landforms trending toward Ungava Bay; these were then preserved under more cold-based subglacial conditions as the ice divide migrated west. When the ice divide was positioned completely west of the study area, east-trending landforms developed under warm-based conditions during flow 3. These varying basal thermal conditions are supported by the more detailed investigation of subglacial conditions in the northern part of the study area (Rice et al., 2020c).

Flow 3 reworked and re-entrained flow 1 dispersal patterns and created palimpsest glacial dispersal patterns across the centre of the study area (e.g. Fig. 19, 20). Regions where flow 1 dispersal fans were reworked are greatest in areas where flow 3 has the most predominant surficial signature (i.e. the highest abundance of east-trending landforms), as shown by the distribution of Cu from the Doublet zone, which indicates flow 3 has reworked flow 1 dispersal to the northeast and re-entrained this material preferentially to the east (Fig. 16). Additional dispersal to the east associated with flow 3 is observed in the dispersal of orthopyroxene grains and felsic clasts from the De Pas batholith. Eastward dispersal was attributed by Klassen and Thompson (1993) to their event II and, in some cases, event IV. The absence of Martin Lake rhyolite clasts within the study area (Rice et al., 2020b) indicates this unique bedrock lithological unit was not dispersed as far as the iron-formation clasts to the east or northeast and suggests that Martin Lake rock units break down and weather more easily than resilient iron-formation clasts.

As ice streaming continued to drain ice from the LIS, the profile of the ice sheet began to lower, leading to more topographic control on ice flows. Within the study area, this can

Figure 18. Proportional-dot map of goethite-grain abundance (normalized to 10 kg) in the 0.25 to 0.5 mm fraction of till samples (*see* Fig. 2 for bedrock geology legend). The source areas for the goethite grains are the iron formations of the Labrador Trough.

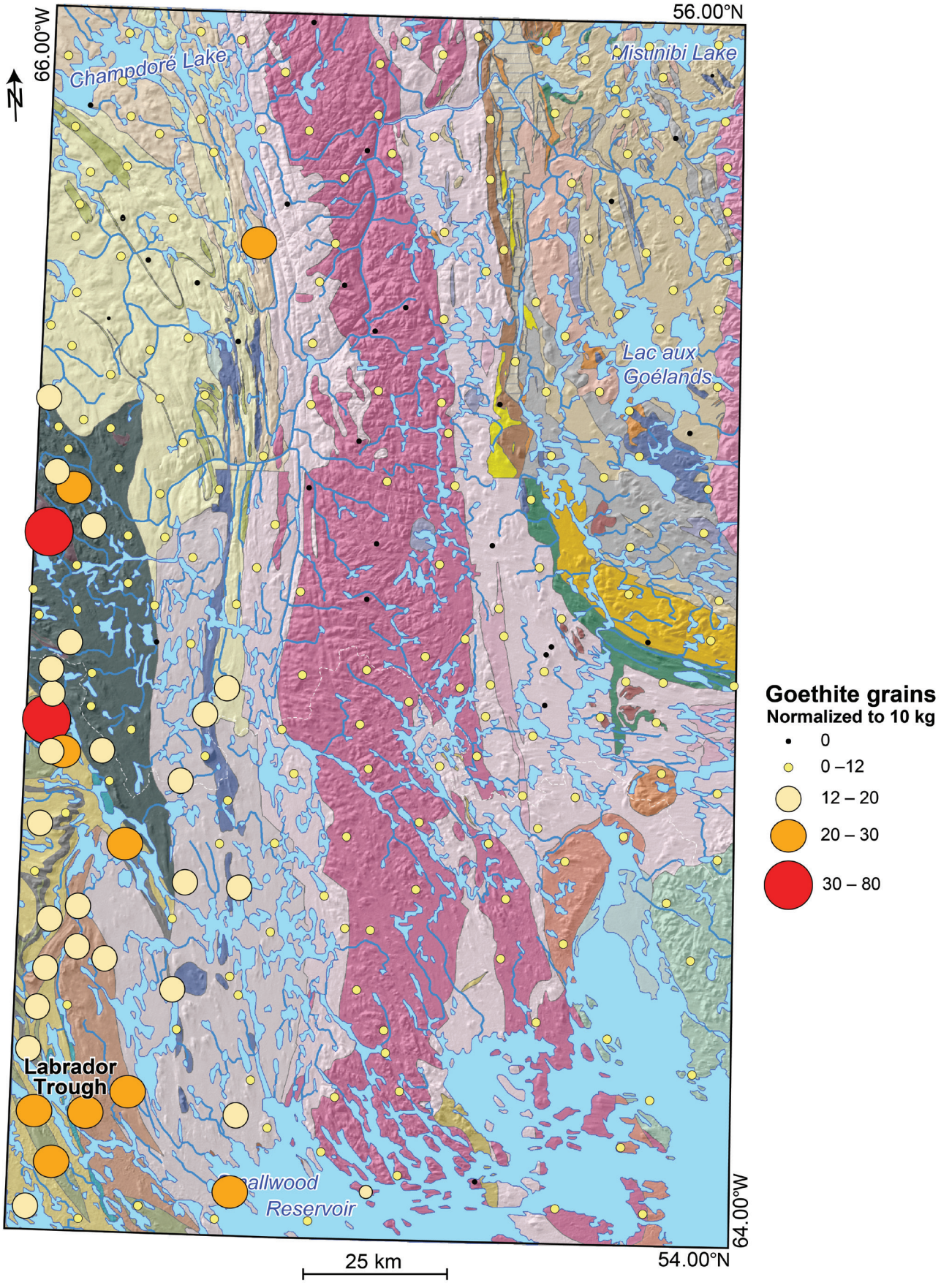
56.00°N
66.00°W
Champdoré Lake
Mistinibi Lake
Lac aux Goélands
Labrador Trough
Reservoir
64.00°W
54.00°N
25 km
Goethite grains
Normalized to 10 kg
0
0 –12
12 – 20
20 – 30
30 – 80

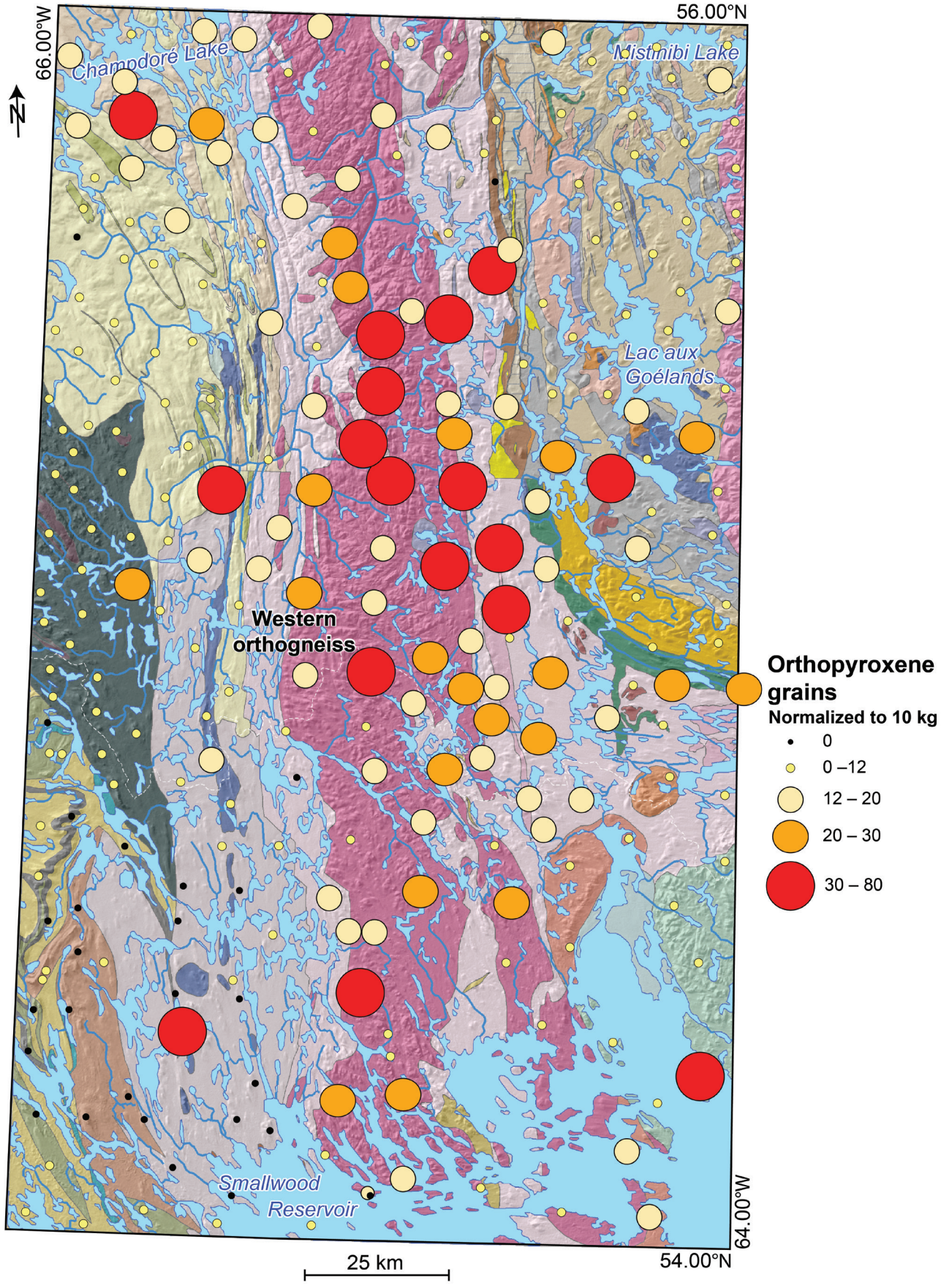
56.00°N
66.00°W
64.00°W
54.00°N
N
Chamodoré Lake
Mistmibi Lake
Lac aux Goélands
Western orthogneiss
Smallwood Reservoir
25 km
Orthopyroxene grains
Normalized to 10 kg
0
0 –12
12 – 20
20 – 30
30 – 80

Figure 19. Proportional-dot map of orthopyroxene-grain abundance (normalized to 10 kg) in the 0.25 to 0.5 mm nonferromagnetic fraction of till samples (*see* Fig. 2 for bedrock geology legend). The source area for the orthopyroxene grains lies within the western orthogneiss.

be observed in the patterns associated with flow 4 striations. Flow 4 was to the south in the west-central part of the study area, bounded by the central uplands to the east. Beyond the southern limit of these central highlands, the ice then continued to flow southeast into the Smallwood Reservoir (Fig. 12). Glacial dispersal patterns that result from this ice-flow phase are less pronounced than those formed by flows 1, 2, and 3, likely due to the absence of a distinct geochemical, indicator-mineral, or lithological signature of clasts within the confines of the ice-flow extent. However, given the abundance of landforms within its footprint, it is highly likely that flow 4 remobilized and re-entrained existing dispersal patterns. Southeast dispersal from the Labrador Trough toward the Smallwood Reservoir is observed for Cu (Fig. 16) and iron-formation clasts (Fig. 20), and, to a lesser degree, orthopyroxene grains (Fig. 19) from the western orthogneiss, although the patterns probably reflect early flow 2 (to the south) or flow 3 (to the east), or a combination of all three flows.

Dispersal patterns related to the youngest ice-flow events regrouped into flow 5 were not observed. Glacial transport was likely minimal, as the ice sheet had thinned and further separated into regions of independent ice flow, with ice flow largely influenced by topography, although the ice-flow phase was generally to the northeast. Additionally, only poorly developed streamlined landforms in a small low-lying area were identified related to this last ice-flow phase, indicating that it was characterized by relatively low erosion and hence had minimal impact on glacial sediment dispersal.

Deglaciation

Deglaciation of the area, based on OSL dating and ^{10}Be surface-exposure ages from this study, and constrained using regionally reported ^{10}Be ages, occurred about 8 ka (Carlson et al., 2007, 2008; Ullman et al., 2016; Dubé-Loubert et al., 2018). Although ^{10}Be samples with relatively high levels of inheritance (moderate ^{10}Be abundances based on regional deglacial timing) are easily identified, those with low inheritance cannot be confidently recognized. Therefore, samples that are only centuries or even a millennium too old will be impossible to identify in the absence of complementary dating (e.g. ^{14}C) of morphostratigraphic controls (i.e. dating landforms that determine ice-margin positions). As the geochronological transect used in this study was devoid of end moraines, there was no way to control the amount of inheritance within the ^{10}Be samples. Furthermore, even if the younger ^{10}Be ages may represent maximum ages, averaging of regional ages is inappropriate. However, when the ^{10}Be ages and OSL dates are examined together (*see* Rice et al., 2019), the overall findings from this study support previous work (Ives, 1960a; Clark et al., 2000) stating the Quebec–Labrador sector was highly fragmented in its late stages and disappeared at approximately 8 ka. They also correlate well with the more recent regional radiocarbon-based deglacial chronology presented by Dalton et al. (2020). In turn, the data from this study suggest the U-shaped boundary, at least at its southeastern extent, developed well before the formation of glacial lakes and therefore had no bearing on ice-margin-retreat patterns. However, topography (DEM data), identification of moraines, geomorphology and the position of moraines, meltwater channels, deglacial ages (OSL), and raised beach ridges are used to interpret ice-margin-retreat patterns and to propose five general phases of glacial lake evolution for the study area. Figure 22 shows a generalized illustration of these phases presented in relative chronological order.

The glacial lake in the southeast of the study area was formally named ‘glacial Lake Low’ during this research project (Paulen et al., 2017). Lake Low formed in the lowland region previously occupied by lakes Ossokmanuan, Lobstick, and Michikamau and now occupied by the Smallwood Reservoir (Fig. 22a). The glacial lake formed as meltwater began to pond in the lowlands, constrained to the south by a drainage divide that must have been somewhere near the headwaters of the Churchill River (Paulen et al., 2020a, b; Fig. 22a). A re-entrant extending from the headwaters of the Churchill River into the lowlands now occupied by the Smallwood Reservoir would allow the occurrence of an ice-free basin hosting Lake Low after 9.0 ka (OSL age for sample 14-PTA-R035; Table 2). This glacial lake required an ice dam blocking the bedrock valleys, or fiords to the east of the study area, to prevent drainage to the Labrador coast. Lake Low formed and subsequently drained prior to northwestward ice-margin retreat over the highlands to the north and west (Fig. 22b–e).

As the ice-sheet margin retreated north and west, meltwater accumulated in the headwaters of the George River valley, north of the paleodrainage divide, which resulted in the formation of glacial Lake Naskaupi (Fig. 22b, c).

Figure 20. Proportional-dot map of iron-formation clasts in the 2 to 50 mm fraction of bulk till samples (*see* Fig. 2 for bedrock geology legend). Iron-formation clasts were derived from the Labrador Trough.

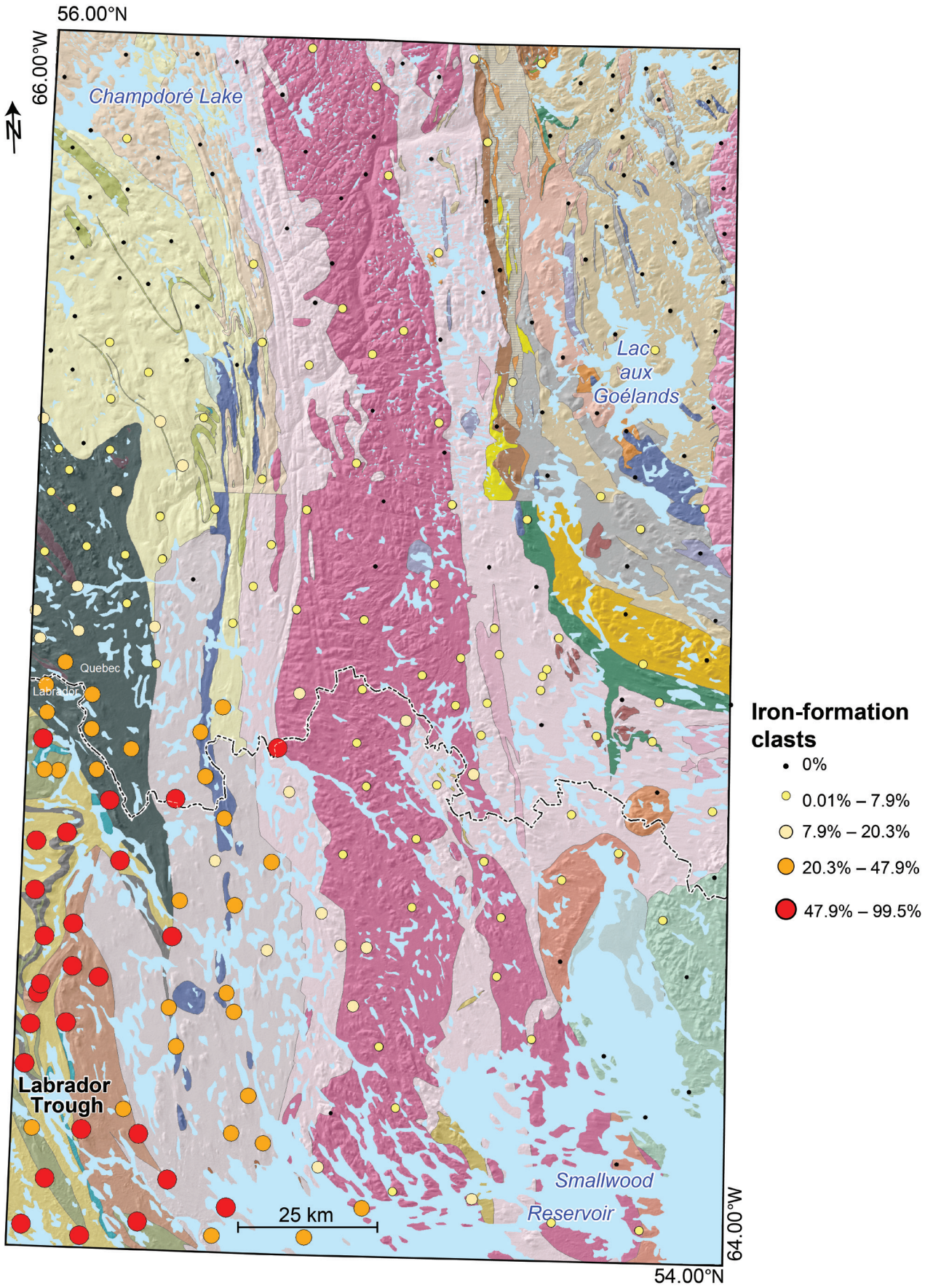
56.00°N
66.00°W
N
Champdoré Lake
Lac aux Goélands
Quebec
Labrador
Labrador Trough
Smallwood Reservoir
25 km
64.00°W
54.00°N
Iron-formation clasts
0%
0.01% – 7.9%
7.9% – 20.3%
20.3% – 47.9%
47.9% – 99.5%

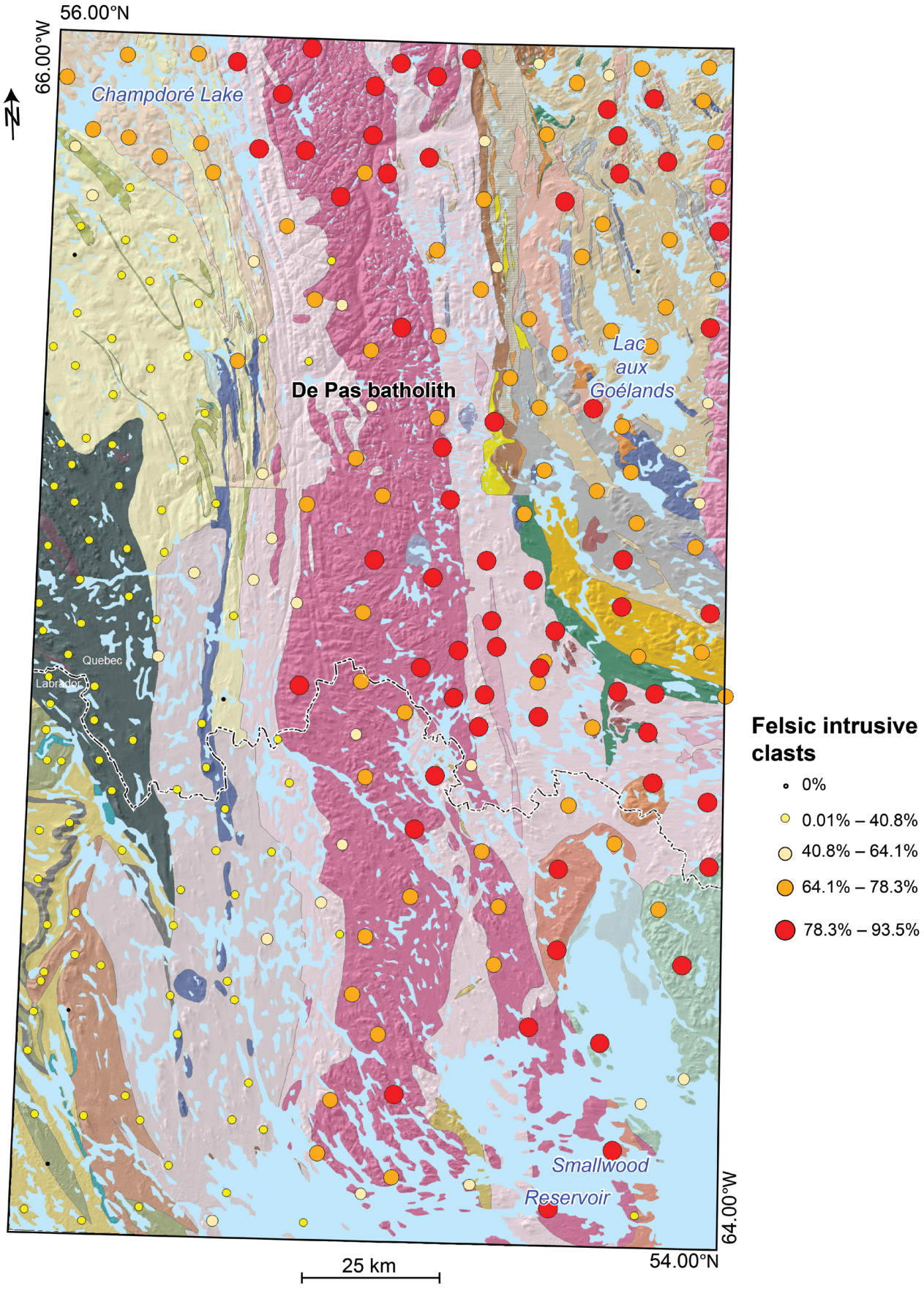
56.00°N
66.00°W
N
Champdoré Lake
De Pas batholith
Lac
aux
Goélands
Quebec
Labrador
Smallwood
Reservoir
64.00°W
54.00°N
25 km
Felsic intrusive clasts
0%
0.01% – 40.8%
40.8% – 64.1%
64.1% – 78.3%
78.3% – 93.5%

Figure 21. Proportional-dot map of felsic intrusive clasts in the 2 to 50 mm fraction of bulk till samples (*see* Fig. 2 for bedrock geology legend). Felsic intrusive clasts were derived from the De Pas batholith.

Within the study area, two samples providing chronology on the maximum (15-PTA-149 at elev. 486 ± 5 m; Table 2) and minimum (15-PTA-074 at elev. 314 ± 5 m; Table 2) levels of Lake Naskaupi yielded ages of 7.93 ± 0.72 and 7.65 ± 0.99 ka, respectively (Fig. 22b, e). As the ice sheet thinned and further fragmented, glacial Lake McLean developed in the lowlands of the Champdoré Lake area and formed beaches at 426 ± 5 m (Fig. 22d). However, the sample collected from that beach of Lake McLean yielded an improbably old age (35.5 ± 4.0 ka); therefore the timing of this lake remains poorly constrained. The DEM data suggest that Lake McLean must have formed when ice was blocking the Rivière De Pas valley, which prevented the lake from draining southeast into a lower phase of Lake Naskaupi.

As the ice continued to melt, overflow channels formed before Lake Naskaupi catastrophically drained, as indicated from evidence reported to the north of the study area (Dubé-Loubert and Roy, 2017). Following the catastrophic drainage of Lake Naskaupi N2 lake level (Dubé-Loubert et al., 2018), a much lower Lake Naskaupi lingered in the George River and Rivière De Pas valleys at approximately 410 m (Fig. 22e). Glaciofluvial terraces, outwash fans, and the termini of meltwater channels were formed at this time. Sample 15-PTA-074, which was collected from an outwash fan terrace on the bank of the George River, indicated a depositional age of 7.65 ± 0.99 ka. This outwash fan is related to Lake Naskaupi at its lowest stage within the study area, as are shorelines and terraces around this elevation (400 m) identified during surficial mapping (Rice et al., 2017a; Paulen et al., 2020b, c). The timing of Lake McLean drainage is unknown, but it likely drained to the northwest along the Rivière à la Baleine valley (Fig. 4), based on available DEM data. Additional OSL ages are required to constrain the timing and paleogeographic reconstruction presented in Figure 22, and higher resolution DEM data would help constrain the overflow or drainage channels. The OSL results on samples of well sorted sands (e.g. 15-PTA-074) yielded better results than samples collected from more poorly sorted sediments (e.g. 15-PTA-052). Thus, samples from lower energy environments with more consistent depositional rates should be favoured for OSL sampling, likely because these environments were less turbid and more readily exposed to sunlight.

SUMMARY

This work established five ice-flow phases with updated chronological constraints from landform and outcrop-scale ice-flow indicators. An early flow to the northeast (flow 1), from an outflow centre somewhere in the Laurentian Highlands, was followed by the development or migration of an ice divide into the eastern half of the study area and a northwest ice-flow phase (flow 2) highly influenced by ice-stream dynamics in Ungava Bay. Changing dynamics in Ungava Bay led to the westward migration of the ice-stream source areas and the concurrent westward migration of the ice divide across the study area, resulting in a more widespread eastward flow (flow 3). Flow 3 is correlated with numerous ice streams generally flowing to the east that operated within, and just beyond, the study area. As the ice sheet continued to thin, ice began to flow south (flow 4), topographically restricted by the central uplands, and feeding into the lowlands where the Smallwood Reservoir ice stream flowed to the east-southeast. Continued ice streaming led to significant ice-sheet thinning that resulted in the youngest ice-flow phase eventually being controlled by fragmented ice caps (flow 5). As the ice margin retreated during deglaciation, three proglacial lakes formed within the study area. The earliest (and previously unmapped) Lake Low formed in the southeast, followed by continued ice-margin retreat and the formation of Lake Naskaupi in the northeast and Lake McLean in the northwest. These lakes were identified by raised beaches and were targeted for OSL sampling, which yielded deglacial ages that correlate with ^{10}Be exposure ages and indicate the region was deglaciated approximately 8000 years ago.

This work clearly shows that the U-shaped boundary between glacially streamlined landforms is the result of contrasting and changing subglacial thermal conditions, as reflected by the varied preservation of landforms on either side, linked to ice-divide migration across the region. As a result of the changing ice-flow patterns and subglacial thermal regimes, glacial dispersal patterns in the area are complex. In this study, the dispersal patterns are shown to be largely the result of broad northeast dispersal during flow 1, reworked by subsequent ice-flow phases restricted to more localized regions. This work also expands the range of previously documented iron-formation erratic dispersal to the northeast by 50 km. Additionally, the conflicting ice-flow chronologies for the region have been resolved, at least within the study area, providing a framework for reconstructing regional ice-flow phases and for interpreting glacial transport with applications to mineral exploration. The timing and pattern of ice-margin retreat have also been refined; however, additional age data would improve the accuracy and resolution of the proposed reconstruction. Overall, this research has provided important insights into the changing subglacial conditions within the inner regions of large ice sheets throughout glaciation.

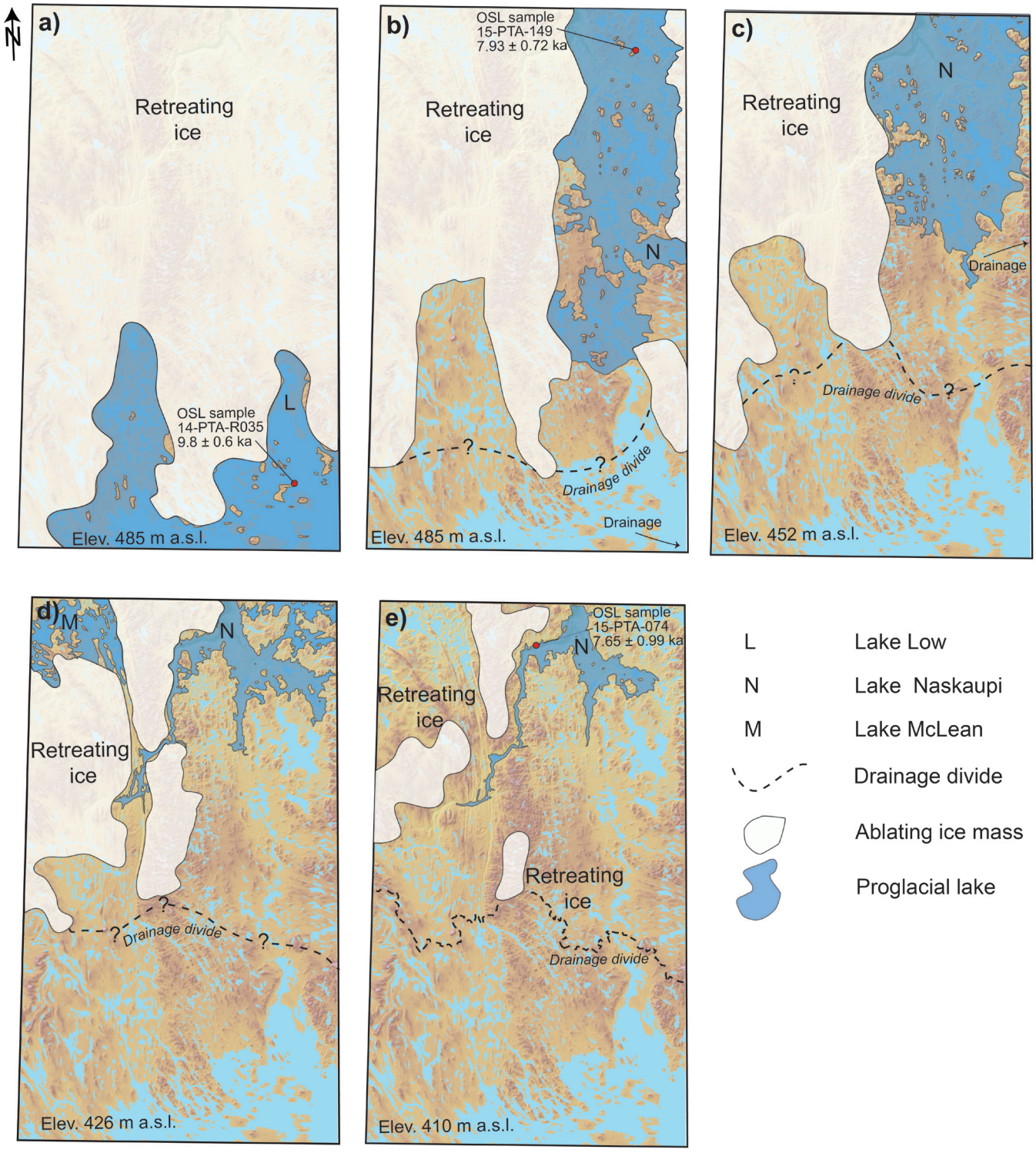

Figure 22. Paleogeographic reconstruction of the three glacial lakes within the study area, constrained by ice-margin retreat, DEM data, and OSL ages from beach sediments and terraced outwash sediments: **a)** initial inundation of the study area by glacial Lake Low as the ice margin retreated north; **b)** a drainage channel somewhere to the east or south drains Lake Low, with meltwater now accumulating north of the drainage divide, forming the early stages of glacial Lake Naskaupi; **c)** continued melting leads to further shrinkage of the ice sheet and a drainage channel is opened up to the east, lowering the level of glacial Lake Naskaupi; **d)** continued melting leads to the formation of glacial Lake McLean in the northwest, while Lake Naskaupi continues to lower; **e)** with deglaciation near complete, Lake McLean has drained to the north and Lake Naskaupi reaches its minimum level. The approximate elevation (elev.) of the lakes is indicated in the bottom left of each relative lake stage.

ACKNOWLEDGMENTS

The Northeast Quebec–Labrador Surficial Mapping activity was carried out as part of the Hudson–Ungava project under the GSC's GEM-2 program in collaboration with the Ministère de l'Énergie et des Ressources naturelles du Québec and the Geological Survey of Newfoundland and Labrador. It was ably managed by Jennifer Bates, Lila Chebab, and Réjean Couture, with support from Ryan Murphy and Daniel Sincennes. The GSC provided financial support to the first author in the form of a bursary through the Government of Canada's Research Affiliate Program. Logistical support for field activities was expertly provided by the Polar Continental Shelf Program (projects no. 059-15 and 060-16) and Norpaq Aviation. The authors thank Gabriel Huot-Vézina (GSC-Québec) and Matt Pyne (GSC-Ottawa) for GIS and database support. Assistance in the field was provided by Grant Hagedorn (University of Waterloo), Alan Lion (University of Ottawa), and Emilie Rufiange (University of Ottawa). Jason Briner (University at Buffalo) and Samuel Kelley (University College Dublin) are thanked for their assistance with ^{10}Be interpretation. The authors are grateful to David Corrigan and Mary Sanborn-Barrie (GSC-Ottawa) for their insights and assistance with related aspects of the bedrock geology. Maxim Gauthier and Alan Rioux (Innokopters Inc.) are thanked for safe transportation and assistance in the field. Pierre-Marc Godbout, Arthur Dyke, and Jean Veillette provided thoughtful comments that greatly improved this manuscript. Isabelle McMartin is thanked for her very hard work as editor of this volume and valuable feedback on this research.

REFERENCES

Aitken, M.J., 1998. An introduction to optical dating; Oxford University Press, 267 p.

Allard, M., Fournier, A., Gahé, E., and Séguin, M.K., 1989. Le Quaternaire de la côte sud-est de la baie d'Ungava, Québec nordique; Géographie physique et Quaternaire, v. 43, p. 325–336. https://doi.org/10.7202/032786ar

Alley, R.B., Cuffey, K.M., and Zoet, L.K., 2019. Glacial erosion: status and outlook; Annals of Glaciology, v. 60, p. 1–13. https://doi.org/10.1017/aog.2019.38

Amor, S., McCurdy, M., and Garrett, R., 2019. Creation of an atlas of lake-sediment geochemistry of western Labrador and northeastern Quebec; Geochemistry: Exploration, Environment, Analysis, v. 19, p. 369–393. https://doi.org/10.1144/geochem2018-061

Argus, D.F., Peltier, W.R., Drummond, R., and Moore, A.W., 2014. The Antarctica component of postglacial rebound model ICE-6G_C (VM5a) based upon GPS positioning, exposure age dating of ice thicknesses, and relative sea level histories; Geophysical Journal International, v. 198, p. 537–563. https://doi.org/10.1093/gji/ggu140

Barnett, D.M., 1967. Glacial Lake McLean and its relationship with glacial Lake Naskaupi; Geographical Bulletin, v. 9, p. 96–101.

Barnett, D.M. and Peterson, J.A., 1964. The significance of glacial Lake Naskaupi 2 in the deglaciation of Labrador–Ungava; The Canadian Geographer / Le Géographe canadien, v. 8, p. 173–181. https://doi.org/10.1111/j.1541-0064.1964.tb00606.x

Bostock, H.S., 2014. Physiographic regions of Canada; Geological Survey of Canada, Map 1254A (second edition), scale 1:5 000 000. https://doi.org/10.4095/293408

Brouard, E. and Lajeunesse, P., 2019. Ice-stream flow switching by up-ice propagation of instabilities along glacial marginal troughs; The Cryosphere, v. 13, p. 981–996. https://doi.org/10.5194/tc-13-981-2019

Brushett, D. and Amor, S., 2013. Kimberlite-indicator mineral analysis of esker samples, western Labrador; Government of Newfoundland and Labrador, Department of Natural Resources, Geological Survey, Open File LAB/1620, 58 p.

Campbell, H.E., Paulen, R.C., and Rice, J.M., 2018. Surficial geology, Ashuanipi River, Newfoundland and Labrador, NTS 23-I southwest; Geological Survey of Canada, Canadian Geoscience Map 346 (preliminary edition), scale 1:100 000. https://doi.org/10.4095/306431

Carlson, A.E., Clark, P.U., Raisbeck, G.M., and Brook, E.J., 2007. Rapid Holocene deglaciation of the Labrador sector of the Laurentide Ice Sheet; Journal of Climate, v. 20, p. 5126–5133. https://doi.org/10.1175/JCLI4273.1

Carlson, A.E., LeGrande, A.N., Oppo, D.W., Came, R.E., Schmidt, G.A., Anslow, F.S., Licciardi, J.M., and Obbink, E.A., 2008. Rapid early Holocene deglaciation of the Laurentide Ice Sheet; Nature Geoscience, v. 1, p. 620–624. https://doi.org/10.1038/ngeo285

Clarhäll, A. and Jansson, K., 2003. Time perspectives on glacial landscape formation — glacial flow chronology at Lac aux Goélands, northeastern Quebec, Canada; Journal of Quaternary Science, v. 18, no. 5, p. 441–452. https://doi.org/10.1002/jqs.763

Clark, P.U. and Fitzhugh, W.W., 1990. Late deglaciation of the central Labrador coast and its implications for the age of glacial lakes Naskaupi and McLean and for prehistory; Quaternary Research, v. 34, no. 3, p. 296–305. https://doi.org/10.1016/0033-5894(90)90042-J

Clark, T. and Wares, M., 2005. Lithotectonic and metallogenic synthesis of the New Quebec Orogen (Labrador Trough); Ministère des Ressources naturelles du Québec, MM 2005-01, 175 p.

Clark, C.D., Knight, J.K., and Gray, J.T., 2000. Geomorphological reconstruction of the Labrador sector of the Laurentide Ice Sheet; Quaternary Science Reviews, v. 19, p. 1343–1366. https://doi.org/10.1016/S0277-3791(99)00098-0

Clark, P.U., Brook, E.J., Raisbeck, G.M., Yiou, F., and Clark, J., 2003. Cosmogenic ^{10}Be ages of the Saglek moraines, Torngat Mountains, Labrador; Geology, v. 31, p. 617–620. https://doi.org/10.1130/0091-7613(2003)031%3c0617:CBAOTS%3e2.0.CO%3b2

Corrigan, D., Van Rooyen, D., Morin, A., Houlé, M.G., and McNicoll, V.J., 2015. Report of activities for the Core Zone and bounding orogens: the New Quebec Orogen and its relationship with the Core Zone in the Kuujjuaq area; Geological Survey of Canada, Open File 7962, 11 p. https://doi.org/10.4095/297404

Corrigan, D., van Rooyen, D., Morin, A., Houlé, M.G., and Bédard, M.-P., 2016. Report of activities for the Core Zone and bounding orogens: recent observations from the New Quebec Orogen in the Schefferville area, Quebec and Labrador, GEM-2 Hudson–Ungava project; Geological Survey of Canada, Open File 8127, 15 p. https://doi.org/10.4095/299249

Corrigan, D., Wodicka, N., McFarlane, C., Lafrance, I., van Rooyen, D., Bandyayera, D., and Bilodeau, C., 2018. Lithotectonic framework of the Core Zone, southeastern Churchill Province, Canada; Geoscience Canada, v. 45, p. 1–24. https://doi.org/10.12789/geocanj.2018.45.128

Cowan, W.R., 1967. The glacial geomorphology of the Shoal Lake area, Labrador; M.Sc. thesis, McGill University, Montréal, Quebec, 127 p.

Dalton, A.S., Margold, M., Stokes, C.R., Tarasov, L., Dyke, A.S., Adams, R.S., Allard, S., Arends, H.E., Atkinson, N., Attig, J.W., Barnett, P.J., Barnett, R.L., Batterson, M., Bernatchez, P., Borns, H.W., Jr., Breckenridge, A., Briner, J.P., Brouard, É., Campbell, J.E., . . . Wright, H.E., Jr., 2020. An updated radiocarbon-based ice margin chronology of the last deglaciation of the North American ice sheet complex; Quaternary Science Reviews, v. 234, art. 106223. https://doi.org/10.1016/j.quascirev.2020.106223

Douglas, M.C.V. and Drummond, R.N., 1955. Map of the physiographic regions of Ungava–Labrador; The Canadian Geographer / Le Géographe canadien, v. 2, p. 9–16. https://doi.org/10.1111/j.1541-0064.1955.tb01746.x

Dubé-Loubert, H., 2019. Dynamique glaciaire et géochronologie du secteur Labrador de l'lnlandsis laurentidien et évolution du lac Naskaupi au cours de la dernière déglaciation; Ph.D. thesis, Université du Québec à Montréal, Montréal, Quebec, 179 p.

Dubé-Loubert, H. and Roy, M., 2017. Development, evolution and drainage of glacial Lake Naskaupi during the deglaciation of north-central Quebec and Labrador; Journal of Quaternary Science, v. 32, p. 1121–1137. https://doi.org/10.1002/jqs.2997

Dubé-Loubert, H., Roy, M., Schaefer, J.M., and Clark, P.U., 2018. ^{10}Be dating of former glacial Lake Naskaupi (Quebec–Labrador) and timing of its discharges during the last deglaciation; Quaternary Science Reviews, v. 191, p. 31–40. https://doi.org/10.1016/j.quascirev.2018.05.008

Dunai, T.J., 2010. Cosmogenic nuclides: principles, concepts, and applications in the Earth surface sciences; Cambridge University Press, 198 p. https://doi.org/10.1017/CBO9780511804519

Dyke, A.S., 2004. An outline of North American deglaciation with emphasis on central and northern Canada; *in* Quaternary glaciations — extent and chronology, part II: North America, (ed.) J. Ehlers and P.L. Gibbard; Developments in Quaternary Sciences, v. 2, part B, p. 371–406.

Dyke, A.S. and Prest, V.K., 1987. Late Wisconsinan and Holocene history of the Laurentide Ice Sheet; Géographie physique et Quaternaire, v. 41, p. 237–263. https://doi.org/10.7202/032681ar

Dyke, A.S., Dredge, L.A., and Vincent, J.-S., 1982. Configuration and dynamics of Laurentide Ice Sheet during the Late Wisconsin maximum; Géographie physique et Quaternaire, v. 36, p. 5–14. https://doi.org/10.7202/032467ar

Dyke, A.S., Morris, T.F., Green, D.E.C., and England, J., 1992. Quaternary geology of Prince of Wales Island, Arctic Canada; Geological Survey of Canada, Memoir 433, 149 p. https://doi.org/10.4095/134058

Fuchs, M. and Owen, L.A., 2008. Luminescence dating of glacial and associated sediment: review, recommendations and future directions; Boreas, v. 37, p. 636–659. https://doi.org/10.1111/j.1502-3885.2008.00052.x

Fulton, R.J., 1995. Surficial materials of Canada / Matériaux superficiels du Canada; Geological Survey of Canada, Map 1880A, scale 1:5 000 000. https://doi.org/10.4095/205040

Fulton, R.J. and Hodgson, D.A., 1979. Wisconsin glacial retreat, southern Labrador; *in* Current research, part C; Geological Survey of Canada, Paper 79-1C, p. 17–21. https://doi.org/10.4095/124066

Gauthier, M.S., Hodder, T.J., Ross, M., Kelley, S.E., Rochester, A., and McCausland, P., 2019. The subglacial mosaic of the Laurentide Ice Sheet; a study of the interior region of southwestern Hudson Bay; Quaternary Science Reviews, v. 214, p. 1–27. https://doi.org/10.1016/j.quascirev.2019.04.015

Gowan, E.J., Niu, L., Knorr, G., and Lohmann, G., 2019. Geology datasets in North America, Greenland and surrounding areas for use with ice sheet models; Earth System Science Data, v. 11, p. 375–391. https://doi.org/10.5194/essd-11-375-2019

Granberg, H.B. and Krishnan, T.K., 1984. Wood remnants 24 250 years old in central Labrador; *in* 5th AQQUA Congress, (ed.) J.-M. Dubois, H. Gwyn, and T. Webb III; Association québécoise pour l'étude du Quaternaire, 4–7 October 1984, Sherbrooke, Quebec, Program and Abstracts, p. 30.

Hall, A.M., Krabbendam, M., van Boeckel, M., Goodfellow, B.W., Hätterstrand, C., Heyman, J., Palamakumbura, R.N., Stroeven, A.P., and Näslund, J.-O., 2020. Glacial ripping: geomorphological evidence from Sweden for a new process of glacial erosion; Geografiska Annaler, Series A, Physical Geography, v. 102, no. 4, p. 333–353. https://doi.org/10.1080/04353676.2020.1774244

Henderson, E.P., 1959. A glacial study of central Quebec–Labrador; Geological Survey of Canada, Bulletin 50, 94 p. https://doi.org/10.4095/123901

Hickin, A.S., Lian, O.V., Levson, V.M., and Cui, Y., 2015. Pattern and chronology of glacial Lake Peace shorelines and implications for isostasy and ice-sheet configuration in northeastern British Columbia, Canada; Boreas, v. 44, p. 288–304. https://doi.org/10.1111/bor.12110

Hillaire-Marcel, C., Occhietti, S., and Vincent, J.-S., 1981. Sakami moraine, Quebec: a 500-km-long moraine without climatic control; Geology, v. 9, no. 5, p. 210–214. https://doi.org/10.1130/0091-7613(1981)9%3c210:SMQAKM%3e2.0.CO%3b2

Hughes, O.L., 1964. Surficial geology, Nichicun–Kaniapiskau map-area, Quebec; Geological Survey of Canada, Bulletin 106, 20 p. https://doi.org/10.4095/100624

Huntley, D.J. and Lamothe, M., 2001. Ubiquity of anomalous fading in K-feldspars and the measurements and correction for it in optical dating; Canadian Journal of Earth Sciences, v. 38, p. 1093–1106. https://doi.org/10.1139/e01-013

Ives, J., 1956. Till patterns in central Labrador; The Canadian Geographer / Le Géographe canadien, v. 2, p. 25–33. https://doi.org/10.1111/j.1541-0064.1956.tb01775.x

Ives, J.D., 1958. Glacial drainage channels as indicators of late-glacial conditions in Labrador–Ungava: a discussion; Cahiers de géographie du Québec, v. 3, p. 57–72. https://doi.org/10.7202/020113ar

Ives, J.D., 1960a. The deglaciation of Labrador–Ungava — an outline; Cahiers de géographie du Québec, v. 4, p. 323–343. https://doi.org/10.7202/020222ar

Ives, J.D., 1960b. Former ice-dammed lakes and the deglaciation of the middle reaches of the George River, Labrador–Ungava; Geographical Bulletin, v. 14, p. 44–69.

James, D.T., Johnston, D.H., and Crisby-Wittle, L., 1993. Geology of the eastern Smallwood Reservoir area, western Labrador; *in* Current research; Newfoundland Department of Mines and Energy, Geological Survey Branch, Report 93-1, p. 35–49.

James, D.T., Connelly, J.N., Wasteneys, H.A., and Kilfoil, G.J., 1996. Paleoproterozic litholotectonic divisions of the southeastern Churchill Province, western Labrador; Canadian Journal of Earth Sciences, v. 33, p. 216–230. https://doi.org/10.1139/e96-019

James, D.T., Nunn, G.A.G., Kamo, S., and Kwok, K., 2003. The southeastern Churchill Province revisited: U-Pb geochronology, regional correlations, and enigmatic Orman Domain; Newfoundland Department of Mines and Energy, Current Research 03-1, p. 35–45.

Jansson, K.N., 2005. Map of the glacial geomorphology of north-central Quebec–Labrador, Canada; Journal of Maps, v. 1, no. 1, p. 46–55. https://doi.org/10.4113/jom.2005.33

Jansson, K.N., Kleman, J., and Marchant, D.R., 2002. The succession of ice-flow pattern in north central Quebec–Labrador, Canada; Quaternary Science Reviews, v. 21, p. 503–523. https://doi.org/10.1016/S0277-3791(01)00013-0

Jansson, K.N., Stroeven, A.P., and Kleman, J., 2003. Configuration and timing of Ungava Bay ice streams, Labrador–Ungava, Canada; Boreas, v. 32, p. 256–262. https://doi.org/10.1111/j.1502-3885.2003.tb01441.x

Kirby, R.P., 1962. Movements of ice in central Labrador–Ungava; Cahiers de géographie du Québec, v. 5, p. 206–218.

Klassen, R.A. and Bolduc, A.M., 1984. Ice flow directions and drift composition, Churchill Falls, Labrador; *in* Current research, part A; Geological Survey of Canada, Paper 84-1A, p. 255–258. https://doi.org/10.4095/119673

Klassen, R.A. and Knight, R.D., 1995. Till geochemistry of central Labrador; Geological Survey of Canada, Open File 3213, 250 p. https://doi.org/10.4095/205763

Klassen, R.A. and Paradis, S., 1990. Surficial geology of western Labrador; Geological Survey of Canada, Open File 2198, scale 1:250 000. https://doi.org/10.4095/130817

Klassen, R.A. and Thompson F.J., 1987. Ice flow history and glacial dispersal in the Labrador Trough; *in* Current research, part A; Geological Survey of Canada, Paper 87-1A, p. 61–71. https://doi.org/10.4095/122511

Klassen, R.A. and Thompson, F.J., 1988. Glacial studies in Labrador; *in* Current research, part C; Geological Survey of Canada, Paper 88-1C, p. 109–116. https://doi.org/10.4095/122622

Klassen, R.A. and Thompson, F.J., 1989. Ice flow history and glacial dispersion patterns, Labrador; *in* Drift prospecting, (ed.) R.N.W. DiLabio and W.B. Coker; Geological Survey of Canada, Paper 89-20, p. 21–29. https://doi.org/10.4095/127361

Klassen, R.A. and Thompson, F.J., 1993. Glacial history, drift composition, and mineral exploration, central Labrador; Geological Survey of Canada, Bulletin 435, 82 p. https://doi.org/10.4095/183906

Klassen, R.A., Matthews, J.V.J., Mott, R.J., and Thompson, F.J., 1988. The stratigraphic and paleobotanical record of interglaciation in the Wabush region of western Labrador; *in* Climatic fluctuations and man 3, (ed.) C.R. Harington; Annual Meeting of the Canadian Committee on Climatic and Man, January 28–29, 1988, Ottawa, Ontario, Program, abstracts and news, p. 24–26 (abstract).

Klassen, R.A., Paradis, S., Bolduc, A.M., and Thomas, R.D., 1992. Glacial landforms and deposits, Labrador, Newfoundland and eastern Quebec / Formes et dépôts glaciaires, Labrador (Terre-Neuve) et est du Québec; Geological Survey of Canada, Map 1814A, scale 1:1 000 000. https://doi.org/10.4095/183872

Kleman, J. and Glasser, N.F., 2007. The subglacial thermal organisation (STO) of ice sheets; Quaternary Science Reviews, v. 26, p. 585–597. https://doi.org/10.1016/j.quascirev.2006.12.010

Kleman, J., Fastook, J., and Stroeven, A.P., 2002. Geologically and geomorphologically constrained numerical model of Laurentide Ice Sheet inception and build-up; Quaternary International, v. 95-96, p. 87–98. https://doi.org/10.1016/S1040-6182(02)00030-7

Lal, D., 1991. Cosmic ray labeling of erosion surfaces: in situ nuclide production rates and erosion models; Earth and Planetary Science Letters, v. 104, p. 424–439. https://doi.org/10.1016/0012-821X(91)90220-C

Lauriol, B. and Gray, J.T., 1987. The decay and disappearance of the Late Wisconsin Ice Sheet in the Ungava Peninsula, northern Quebec, Canada; Arctic and Alpine Research, v. 19, no. 2, p. 109–126. https://doi.org/10.2307/1551245

Lepper, K., Buell, A.W., Fisher, T.G., and Lowell, T.V., 2013. A chronology for glacial Lake Agassiz along Upham's namesake transect; Quaternary Research, v. 80, p. 88–98. https://doi.org/10.1016/j.yqres.2013.02.002

Lifton, N., Sayo, T., and Dunai, T.J., 2014. Scaling in situ cosmogenic nuclide production rates using analytical approximations to atmospheric cosmic-ray fluxes; Earth and Planetary Science Letters, v. 386, p. 149–160. https://doi.org/10.1016/j.epsl.2013.10.052

Liverman, D. and Vatcher, H., 1992. Surficial geology of the Cavers and Hollinger Lake areas (NTS 23J/9 and 16); *in* Current research; Government of Newfoundland and Labrador, Department of Mines and Energy, Geological Survey Branch, Report 93-1, p. 127–138.

Liverman, D. and Vatcher, H., 1993. Surficial geology of the Schefferville area (Labrador parts of NTS 23J/10 and 23J/15); *in* Current research; Government of Newfoundland and Labrador, Department of Mines and Energy, Geological Survey Branch, Report 92-1, p. 27–37.

Low, A.P., 1896. Report on explorations in the Labrador Peninsula along the east Main, Koksoak, Hamilton, Manicuagan and portions of other rivers in 1892-93-94-95; Geological Survey of Canada, Annual Report, v. 8, part L, 387 p. https://doi.org/10.4095/293888

Margold, M., Stokes, C.R., Clark, C.D., and Kleman, J., 2015. Ice streams in the Laurentide Ice Sheet: a new mapping inventory; Journal of Maps, v. 11, p. 380–395. https://doi.org/10.1080/17445647.2014.912036

Margold, M., Stokes, C.R., and Clark, C.D., 2018. Reconciling records of ice streaming and ice margin retreat to produce a paleographic reconstruction of the deglaciation of the Laurentide Ice Sheet; Quaternary Science Reviews, v. 189, p. 1–30. https://doi.org/10.1016/j.quascirev.2018.03.013

Marquette, G.C., Gray, J.T., Gosse, J.T., Courchesne, F., Stockli, L., Macpherson, G., and Finkle, R., 2004. Felsenmeer persistence under non-erosive ice in the Torngat and Kaumajet mountains, Quebec and Labrador, as determined by soil weathering and cosmogenic nuclide exposure dating; Canadian Journal of Earth Sciences, v. 41, p. 19–38. https://doi.org/10.1139/e03-072

Mathewes, R.W., Lian, O.B., Clague, J.J., and Huntley, M.J.W., 2015. Early Wisconsinan (MIS 4) glaciation on Haida Gwaii, British Columbia, and implications for biological refugia; Canadian Journal of Earth Sciences, v. 52, p. 939–951. https://doi.org/10.1139/cjes-2015-0041

Matthews, B., 1961. Late Quaternary land emergence in northern Ungava, Quebec; Arctic, v. 20, p. 176–202.

McClenaghan, M.B., Plouffe, A., McMartin, I., Campbell, J.E., Spirito, W.A., Paulen, R.C., Garrett, R.G., and Hall, G.E.M., 2013. Till sampling and geochemical analytical protocols used by the Geological Survey of Canada; Geochemistry: Exploration, Environment, Analysis, v. 13, p. 285–301. https://doi.org/10.1144/geochem2011-083

McClenaghan, M.B., Paulen, R.C., Rice, J.M., Pyne, M., and Lion, A., 2016a. Till geochemical data for the south Core Zone, Quebec and Labrador (NTS 23-P and 23-I): till samples collected in 2014; Geological Survey of Canada, Open File 7967, 32 p. https://doi.org/10.4095/297796

McClenaghan, M.B., Paulen, R.C., and Rice, J.M., 2016b. Indicator mineral abundance data for till samples from the south Core Zone, Quebec and Labrador (NTS 23-P and 23-I): samples collected in 2014; Geological Survey of Canada, Open File 7968, 13 p. https://doi.org/10.4095/297379

McClenaghan, M.B., Paulen, R.C., Rice, J.M., Campbell, H.E., and Pyne, M.D., 2017. Gold grains in till samples from the southern Core Zone, Quebec and Newfoundland and Labrador (NTS 23-P and 23-I): potential for undiscovered mineralization; Geological Survey of Canada, Open File 8222, 21 p. https://doi.org/10.4095/300657

McClenaghan, M.B., Spirito, M.B., Plouffe, W.A., McMartin, A., Campbell, I., Paulen, R.C., Garrett, R.G., Hall, G.E.M., Pelchat, P., and Gauthier, M.S., 2020. Geological Survey of Canada till-sampling and analytical protocols: from field to archive, 2020 update; Geological Survey of Canada, Open File 8591, 73 p. https://doi.org/10.4095/326162

McMartin, I. and Paulen, R.P., 2009. Ice-flow indicators and the importance of ice-flow mapping for drift prospecting; *in* Application of till and stream sediment heavy mineral and geochemical methods to mineral exploration in western and northern Canada, (ed.) R.C Paulen and I. McMartin; Geological Association of Canada, Short Course Notes 18, p. 15–34.

Melanson, A., Bell, T., and Tarasov, L., 2013. Numerical modelling of subglacial erosion and sediment transport and its application to the North American ice sheets over the last glacial cycle; Quaternary Science Reviews, v. 68, p. 154–174. https://doi.org/10.1016/j.quascirev.2013.02.017

Neal, H.E., 2000. Iron deposits of the Labrador Trough; Exploration and Mining Geology, v. 9, p. 113–121. https://doi.org/10.2113/0090113

Occhietti, S., Govare, É., Klassen, R., Parent, M., and Vincent, J.-S., 2004. Late Wisconsin–Early Holocene deglaciation of Quebec–Labrador; *in* Quaternary glaciations — extent and chronology, part II: North America, (ed.) J. Ehlers and P.L. Gibbard; Developments in Quaternary Sciences, v. 2, part B, p. 243–273. https://doi.org/10.1016/S1571-0866(04)80202-1

Paulen, R.C., Rice, J.M., and McClenaghan, M.B., 2015. Streamlined and lobate landforms, relating to successive ice flows in the Smallwood Reservoir, northern Labrador; Joint Assembly 2015 — AGU–GAC–MAC–CGU; Geological Association of Canada–Mineralogical Association of Canada, 3–7 May 2015, Montréal, Quebec (poster).

Paulen, R.C., Rice, J.M., and McClenaghan, M.B., 2017. Surficial geology, northwest Smallwood Reservoir, Newfoundland and Labrador, NTS 23-I southeast; Geological Survey of Canada, Canadian Geoscience Map 315 (preliminary edition), scale 1:100 000. https://doi.org/10.4095/300685

Paulen, R.C., Rice, J.M., and Ross, M., 2019a. Surficial geology, Adelaide Lake, Newfoundland and Labrador–Quebec, NTS 23-I northeast; Geological Survey of Canada, Canadian Geoscience Map 395, scale 1:100 000. https://doi.org/10.4095/313655

Paulen, R.C., Rice, J.M., Campbell, H.E., and McClenaghan, M.B., 2019b. Surficial geology, Knox Lake, Newfoundland and Labrador–Quebec, NTS 23-I northwest; Geological Survey of Canada, Canadian Geoscience Map 377, scale 1:100 000. https://doi.org/10.4095/313547

Paulen, R.C., Rice, J.M., Ross, M., and Lian, O.B., 2020a. Glacial Lake Low: a previously unidentified proglacial lake in western Labrador; GSA 2020 Connects Online, Geological Society of America, Abstracts with Programs, v. 52, no. 6. https://doi.org/10.1130/abs/2020AM-358203

Paulen, R.C., Rice, J.M., Ross, M., and Lian, O.B., 2020b. Timing and paleogeographic reconstruction of glacial Lake Low in western Labrador; GeoConvention 2020, GAC–MAC–IAH–CSPG–CSEG–CWLS, September 21–23, 2020, Calgary, Alberta, extended abstract, 4 p.

Paulen, R.C., Rice, J.M., and Ross, M., 2020c. Surficial geology, Lac Laporte, Quebec, NTS 23-P southwest; Geological Survey of Canada, Canadian Geoscience Map 410, scale 1:100 000. https://doi.org/10.4095/314756

Paulen, R.C., Rice, J.M., and Ross, M., 2020d. Surficial geology, Lac aux Goélands, Quebec, NTS 23-P southeast; Geological Survey of Canada, Canadian Geoscience Map 429, scale 1:100 000.

Peltier, W.R., Argus, D.F., and Drummond, R., 2015. Space geodesy constrains ice age terminal deglaciation: the global Ice-6G_C (VM5a) model; Journal of Geophysical Research: Solid Earth, v. 120, p. 450–487. https://doi.org/10.1002/2014JB011176

Peterson, J.A., 1965. Deglaciation of the Whitegull Lake area, Labrador–Ungava; Cahiers de géographie du Québec, v. 9, p. 183–196. https://doi.org/10.7202/020596ar

Plouffe, A., McClenaghan, M.B., Paulen, R.C., McMartin, I., Campbell, J.E., and Spirito, W.A., 2013. Processing of unconsolidated glacial sediments for the recovery of indicator minerals: protocols used at the Geological Survey of Canada; Geochemistry: Exploration, Environment, Analysis, v. 13, p. 303–316. https://doi.org/10.1144/geochem2011-109

Prest, V.K., 1970. Quaternary geology of Canada; *in* Geology and economic minerals of Canada, (ed.) R.J.W. Douglas; Geological Survey of Canada, Economic Geology Report 1 (fifth edition), p. 675–764. https://doi.org/10.4095/106155

Prichart, H.H., 1911. Through trackless Labrador — with a chapter on fishing by G.M. Gathorne-Hardy; Sturgis and Walton, New York, New York, 254 p.

Refsnider, K.A. and Miller, G.H., 2010. Reorganization of ice sheet flow patterns in Arctic Canada and the mid-Pleistocene transition; Geophysical Research Letters, v. 37, 5 p. https://doi.org/10.1029/2010GL043478

Reyes, A., Dillman, T., Kennedy, K., Froese, D., Beaudoin, A.B., and Paulen, R.C., 2020. Legacy radiocarbon ages and the MIS 3 dating game: a cautionary tale from re-dating of pre-LGM sites in Western Canada; GSA 2020 Connects Online, Geological Society of America, Abstracts with Programs, v. 52, no. 6. https://doi.org/10.1130/abs/2020AM-360064

Rice, J.M., McClenaghan, M.B., Paulen, R.C., Pyne, M.D., and Ross, M., 2017a. Till geochemical data for the southern Core Zone, Quebec and Newfoundland and Labrador (NTS 23-P and 23-I): samples collected in 2015 and 2016; Geological Survey of Canada, Open File 8219, 37 p. https://doi.org/10.4095/304280

Rice, J.M., McClenaghan, M.B., Paulen, R.C., Ross, M., Pyne, M.D., and Lion, A.J., 2017b. Indicator mineral abundance data for till samples from the south Core Zone, Quebec and Labrador (NTS 23-P and 23-I): samples collected in 2015; Geological Survey of Canada, Open File 8187, 19 p. https://doi.org/10.4095/299683

Rice, J.M., Paulen, R.C., and Ross, M., 2017c. Surficial geology, Rivière De Pas, Quebec, NTS 23-P northwest; Geological Survey of Canada, Canadian Geoscience Map 333 (preliminary edition), scale 1:100 000. https://doi.org/10.4095/306166

Rice, J.M., Paulen, R.C., and Ross, M., 2017d. Surficial geology, Lac Mistinibi, Quebec, NTS 23-P northeast; Geological Survey of Canada, Canadian Geoscience Map 316 (preliminary edition), scale 1:100 000. https://doi.org/10.4095/300656

Rice, J.M., Ross, M., Paulen, R.C., Kelley, S.E., Briner, J.P., Neudorf, C.M., and Lian, O.B., 2019. Refining the ice flow chronology and subglacial dynamics across the migrating Labrador divide of the Laurentide Ice Sheet with age constraints on deglaciation; Journal of Quaternary Science, v. 34, p. 519–535. https://doi.org/10.1002/jqs.3138

Rice, J.M., McClenaghan, M.B., Paulen, R.C., Pyne, M.D., Ross, M., and Campbell, H.E., 2020a. Field data for till samples collected in 2014, 2015, and 2016 in the southern Core Zone, Quebec and Labrador (NTS 23-P and 23-I); Geological Survey of Canada, Open File 8655, 11 p. https://doi.org/10.4095/321471

Rice, J.M., Paulen, R.C., Ross, M., and McClenaghan, M.B., 2020b. Clast-lithology data from the southern Core Zone, Quebec and Newfoundland and Labrador (NTS 23-I and 23-P); Geological Survey of Canada, Open File 8721, 14 p. https://doi.org/10.4095/326083

Rice, J.M., Ross, M., Paulen, R.C., Kelley, S.E., and Briner, J.P., 2020c. A GIS-based multi-proxy analysis of the evolution of subglacial dynamics of the Quebec–Labrador ice dome, northeastern Quebec, Canada; Earth Surface Processes and Landforms, v. 45, no. 13, p. 3155–3177. https://doi.org/10.1002/esp.4957

Rice, J.M., Ross, M., and Paulen, R.C., 2020d. The Cabot Lake ice stream: a paleo-ice stream near the Ancestral Labrador ice divide of the Laurentide Ice Sheet's Quebec–Labrador dome; Geological Survey of Canada, Scientific Presentation 109, poster. https://doi.org/10.4095/321077

Ross, M., Campbell, J.E., Parent, M., and Adams, R.S., 2009. Paleo-ice streams and the subglacial mosaic of the North American mid-continental prairies; Boreas, v. 38, p. 421–439. https://doi.org/10.1111/j.1502-3885.2009.00082.x

Roy, M., Veillette, J., Daubois, V., and Ménard, M., 2015. Late-stage phases of glacial Lake Ojibway in the central Abitibi region, eastern Canada; Geomorphology, v. 248, p. 14–23. https://doi.org/10.1016/j.geomorph.2015.07.026

Sanborn-Barrie, M., 2016. Refining lithological and structural understanding of the southern Core Zone, northern Quebec and Labrador in support of mineral resource assessment; Geological Survey of Canada, Open File 7956, 39 p. https://doi.org/10.4095/297560

Short, S.K., 1981. Radiocarbon date list I: Labrador and northern Quebec, Canada; Institution of Arctic and Alpine Research, Occasional Paper 36, p. 1–33.

Smith, S., 2010. Trends in permafrost conditions and the ecology in northern Canada; Canadian Biodiversity: Ecosystem Status and Trends 2010, Technical Thematic Report No. 9; Canadian Councils of Resource Ministers, Ottawa, 27 p.

Staiger, J.W., Gosse, J., Little, E.C., Utting, D.J., Finkel, R., Johnson, J.V., and Fastook, J., 2006. Glacial erosion and sediment dispersion from detrital cosmogenic nuclide analyses of till; Quaternary Geochronology, v. 1, p. 29–42. https://doi.org/10.1016/j.quageo.2006.06.009

Stokes, C.R. and Clark, C.D., 2001. Paleo-ice streams; Quaternary Science Reviews, v. 20, p. 1437–1457. https://doi.org/10.1016/S0277-3791(01)00003-8

Stokes, C.R., Tarasov, L., and Dyke, A.S., 2012. Dynamics of the North American ice sheet complex during its inception and build-up to the last glacial maximum; Quaternary Science Reviews, v. 50, p. 86–104. https://doi.org/10.1016/j.quascirev.2012.07.009

Stone, J.O., 2000. Air pressure and cosmogenic isotope production; Journal of Geophysical Research, v. 105, p. 23753–23759. https://doi.org/10.1029/2000JB900181

Tanner, V., 1947. Outlines of the geography, life and customs of Newfoundland–Labrador (the eastern part of the Labrador Peninsula); Cambridge University Press, 906 p. (2 volumes).

Tarasov, L. and Peltier, W.R., 2004. A geophysically constrained large ensemble analysis of the deglacial history of the North American ice-sheet complex; Quaternary Science Reviews, v. 23, no. 3-4, p. 359–388. https://doi.org/10.1016/j.quascirev.2003.08.004

Ullman, D.J., Carlson, A.E., Anslow, F.S., LeGrande, A.N., and Licciardi, J.M., 2015. Laurentide ice-sheet instability during the last deglaciation; Nature Geoscience, v. 8, p. 534–537. https://doi.org/10.1038/ngeo2463

Ullman, D.J., Carlson, A.E., Hostetler, S.W., Clark, P.U., Cuzzone, J., Milne, G.A., Winsor, K., and Caffee, M., 2016. Final Laurentide ice-sheet deglaciation and Holocene climate-sea level change; Quaternary Science Reviews, v. 152, p. 49–59. https://doi.org/10.1016/j.quascirev.2016.09.014

van der Leeden, J., Belanger, M., Danis, D., Girard, R., and Martelain, J., 1990. Lithotectonic domains in the high-grade terrain east of the Labrador Trough, Quebec; *in* The early Proterozoic trans-Hudson Orogen of North America, (ed.) J.F. Lewry and M.R. Stauffer; Geological Association of Canada, Special Paper 37, p. 371–386.

Veillette, J.J. and Roy, M., 1995. The spectacular cross-striated outcrops of James Bay, Quebec; *in* Current research 1995-C; Geological Survey of Canada, p. 243–248. https://doi.org/10.4095/202923

Veillette, J.J., Dyke, A.S., and Roy, M., 1999. Ice-flow evolution of the Labrador sector of the Laurentide Ice Sheet: a review, with new evidence from northern Quebec; Quaternary Science Reviews, v. 18, p. 993–1019. https://doi.org/10.1016/S0277-3791(98)00076-6

Vincent, J.-S., 1989. Quaternary geology of the southeastern Canadian Shield; *in* Chapter 3 of Quaternary geology of Canada and Greenland, (ed.) R.J. Fulton; Geological Survey of Canada, Geology of Canada, no. 1, p. 249–275 (also Geological Society of America, The Geology of North America, v. K-1, p. 249–275). https://doi.org/10.4095/127971

Wallace, W.S., 1932. John McLean's notes of a twenty-five year's service in the Hudson's Bay Territory; Publications of the Champlain Society, Toronto, Ontario, v. 19, 402 p.

Wardle, R.J. (comp.), 1982a. Geology of the south-central Labrador Trough — Map 1; Government of Newfoundland and Labrador, Department of Mines and Energy, Mineral Development Division, Maps 82-5, scale 1:100 000.

Wardle, R.J. (comp.), 1982b. Geology of the south-central Labrador Trough — Map 2; Government of Newfoundland and Labrador, Department of Mines and Energy, Mineral Development Division, Maps 82-6, scale 1:100 000.

Wardle, R.J., James, D.T., and Hall, J., 2002. The southeastern Churchill Province: synthesis of a Paleoproterozoic transpressional orogen; Canadian Journal of Earth Sciences, v. 39, p. 639–663. https://doi.org/10.1139/e02-004

Wilson, J.T., Drummond, R.N., and Douglas, M.C.V., 1953. Terrain analysis, aps (air photo interpretation); Transactions of the Royal Society of Canada, v. 47, no. 1, p. 11–16.

Young, N.E., Schaeffer, J.M., Briner, J.P., and Goehring, B.M., 2013. A ^{10}Be production-rate calibration for the Arctic; Journal of Quaternary Science, v. 28, p. 515–526. https://doi.org/10.1002/jqs.2642

Appendix A

List of analysis results from GEM-2 Northeast Quebec–Labrador Surficial Mapping activity

Table A1. List of analysis results and published reports from the Northeast Quebec–Labrador Surficial Mapping activity of the Hudson–Ungava project carried out during the second phase of the Geo-mapping for Energy and Minerals program.

Year	Publication	Description	DOI
2014	OF 7705	Report of activities for Core Zone 2014: surficial geology, geochemistry, bedrock mapping	10.4095/295521
2015	OF 7946	Report of activities for Core Zone 2015: surficial geology, geochemistry, gamma-ray spectrometry	10.4095/297388
2016	OF 7967	Till-matrix geochemistry results from samples collected in 2014	10.4095/297796
2016	OF 7968	Indicator-mineral results from samples collected in 2014	10.4095/297379
2016	OF 8148	Report of activities for Core Zone 2016: surficial geology, geochemistry, bedrock mapping	10.4095/299295
2017	OF 8187	Indicator-mineral results from samples collected in 2015	10.4095/299683
2017	CGM 333	Surficial geology map of NTS 23-P northwest	10.4095/306166
2017	OF 8331	Report of activities for Core Zone 2017: surficial geology, geochemistry, gamma-ray spectrometry	10.4095/306137
2017	OF 8219	Till-matrix geochemistry results from samples collected in 2015 and 2016	10.4095/304280
2017	CGM 315	Surficial geology map of NTS 23-I southeast	10.4095/300685
2017	CGM 316	Surficial geology map of NTS 23-P northeast	10.4095/300656
2017	OF 8222	Gold grains from till samples collected in Core Zone, potential for undiscovered mineralization	10.4095/300657
2017	NL DNR CR 17:119–134	Quaternary mapping and till geochemistry in western Labrador	ESS Cont. # 20160333
2018	CGM 346	Surficial geology map of NTS 21-I southwest	10.4095/306431
2018	OF 8337	Radiometric data for NTS 23-I and 23-P	10.4095/308209
2019	JQS, 34:1–17	Ice-flow chronology and subglacial conditions across 23-P north, with constraints on deglaciation	10.1002/jqs.3138
2019	CGM 395	Surficial geology map of NTS 23-I northeast	10.4095/313655
2019	CGM 377	Surficial geology map of NTS 23-I northwest	10.4095/313547
2020	OF 8655	Field data for till samples collected in 2014, 2015, and 2016	10.4095/321471
2020	OF 8721	Clast-lithology data for till samples collected in 2014, 2015, and 2016	10.4095/326083
2020	CGM 410	Surficial geology map of NTS 23-P southwest	10.4095/14756